ORKUSTOFNUN
NATIONAL ENERGY AUTHORITY
GEOTHERMAL DIVISION

# Geothermal Resistivity Survey in the Asal Rift in Djibouti

## Volume I: Main text

Knútur Árnason, Grímur Björnsson, Ólafur G. Flóvenz and Einar H. Haraldsson

**Prepared for the UND-OPS and ISERST**

OS-88031/JHD-05 September 1988

ORKUSTOFNUN - National Energy Authority of Iceland
Geothermal Division

# Geothermal Resistivity Survey in the Asal Rift in Djibouti

## Volume I: Main text

Knútur Árnason, Grímur Björnsson, Ólafur G. Flóvenz and Einar H. Haraldsson

**Prepared for the UND-OPS and ISERST**

OS-88031/JHD-05 September 1988

## ABSTRACT

A total of 45 time-domain electromagnetic (TEM) soundings were made by Orkustofnun (The National Energy Authority of Iceland) in the Asal Rift in Djibouti in June 1988. The purpose of this survey was to obtain information on the resistivity structure in the central Asal Rift for investigation of the geothermal activity in this area.

The main result of the TEM-survey is that there exists an upflow zone of geothermal fluid under Lava Lake. This is reflected in the resistivity structure below Lava Lake by a local updoming of the water table above sea level and by the absence of high resistivity at depth within the phyllic zone caused by high temperatures. A sudden drop in the water table is observed along a narrow belt crossing the central Asal Rift between the borehole Asal-5 and Lava Lake. This implies a low permeability zone, which is probably due to self-sealing of the geothermal system under Lava Lake caused by precipitation of secondary minerals.

At shallow depth, but below the groundwater level under Lava Lake, the resistivity is furthermore higher than at similar depths in the surrounding area. This indicates a lower porosity due to secondary mineralization, i.e. a kind of a cap rock above the geothermal upflow zone.

It is recommended that one or two exploratory wells be drilled within Lava Lake to a depth of at least 800 m so that the existence of the geothermal upflow zone can be verified. It is important to site the wells in such a way that they will intersect faults or fractures since permeability is likely to be very low except where it is maintained by recent tectonic activity.

CONTENTS


ABSTRACT 2

1. INTRODUCTION 4

2. FIELDWORK 4

3. DATA PROCESSING AND INVERSION 6

4. INTERPRETATION OF THE DATA 9
   4.1 The layering of the resistivity 9
   4.2 Cross sections 12
   4.3 The physical meaning of the resistivity layers 13
      4.3.1 General comments on the dependence of resistivity on other parameters 13
      4.3.2 The data from the boreholes 15
      4.3.3 Conclusions on the nature of resistivity boundaries in the Asal Rift 17
   4.4 The water table 18
   4.5 Isoresistivity maps 19

5. CONCLUSIONS AND A MODEL OF THE GEOTHERMAL ACTIVITY IN THE CENTRAL ASAL RIFT 20

6. RECOMMENDATIONS 22

7. SOURCES OF INFORMATION 23

FIGURES 25

# 1. INTRODUCTION

In a telex dated April 6, the Djibouti Geothermal Project Manager Mr. Ísleifur Jónsson asked Orkustofnun (National Energy Authority of Iceland) to make a cost estimate and an offer for a resistivity survey in the Lava Lake area in the central Asal Rift in Djibouti. The survey was to be paid by the UNDP. The objective of the survey should be to locate possible geothermal resources in the central rift and should be carried out as soon as possible.

Orkustofnun responded in a telex dated April 13, proposing a loop-loop TEM resistivity survey. The TEM method was proposed because of the arid condition in the prospect area. This method does not require transmission of electrical current into the ground as most other controlled source resistivity methods do. The proposal comprised 5 weeks of fieldwork and data collection, starting in late May, followed by 6 weeks of inversion and interpretation of the measured data and reporting.

The Orkustofnun's offer was accepted and preparation for the field mission was initiated in the middle of April. The Icelandic survey team arrived in Djibouti on May 29 and data collection started June 3. At the end of the field work on July 3 a progress report was delivered to the ISERST and UNDP offices in Djibouti.

This is the final report on the resistivity survey, and is divided into two volumes. Volume one contains the main text describing the field work and inversion of the collected data. Included is an integrated interpretation of the resistivity structure of the prospected area, as revealed by the survey, which is made on the basis of other relevant data from the area. A conceptual model of a geothermal system in the central Asal Rift is also proposed. Volume two contains a short technical description of the survey method, data collection, data processing and inversion. It also contains a listing of the data collected and the resulting apparent resistivity curves along with the resistivity models obtained by one-dimensional inversion of the curves.

In addition to the resistivity data obtained during this survey a great deal of other information was used directly and indirectly to constrain the interpretation of the TEM-soundings and to support the proposed conceptual model of the geothermal field. The sources of information are listed in section 7.

# 2. FIELDWORK

The three Icelandic field crew members arrived in Djibouti in the evening of May 29. After four days of preparation and clearing the survey equipment through customs the equipment was taken to the field camp in the prospect area. Field work started on June 3 and was finished on June 30. The progress of the field work is summarized in table 1.

The field work was carried out with only two interruptions. The field team attended a science-review meeting at ISERST's headquarters on June 14 and June 27, the national holiday of Djibouti, was observed. In addition, two short trips were made to the city of Djibouti.

| Day | Activity |
|---|---|
| 28.5. | Traveling from Iceland to Djibouti |
| 29.5. | ---- - --- - --- |
| 30.5. | Preparation in Djibouti |
| 31.5. | Preparation and trip to prospect area |
| 1.6. | Preparation in Djibouti |
| 2.6. | Preparation and moving to field camp |
| 3.6. | Measured station DJ-01 |
| 4.6. | --- --- DJ-02 |
| 5.6. | --- --- DJ-03 |
| 6.6. | Measured stations DJ-04 and DJ-05 |
| 7.6. | --- --- DJ-06 - DJ-07 |
| 8.6. | Measured station DJ-08, trip to Djibouti |
| 9.6. | Measured stations DJ-09 and DJ-10 |
| 10.6. | --- --- DJ-11 - DJ-12 |
| 11.6. | --- --- DJ-13 - DJ-14 |
| 12.6. | --- --- DJ-15 - DJ-16 |
| 13.6. | --- --- DJ-17 |
| 14.6. | Attended science meeting at ISERST and presented preliminary results |
| 15.6. | Measured stations DJ-18 and DJ-19 |
| 16.6. | --- --- DJ-20 - DJ-21 |
| 17.6. | --- --- DJ-22 - DJ-23 |
| 18.6. | --- --- DJ-24 - DJ-25 |
| 19.6. | --- --- DJ-26 - DJ-27 |
| 20.6. | --- --- DJ-28 - DJ-29 |
| 21.6. | --- --- DJ-30 - DJ-31 |
| 22.6. | --- --- DJ-32 |
| 23.6. | --- --- DJ-33 - DJ-34 |
| 24.6. | --- --- DJ-35 - DJ-36 |
| 25.6. | --- --- DJ-37 - DJ-38 |
| 26.6. | --- --- DJ-39 - DJ-40 |
| 27.6. | Day off |
| 28.6. | Measured station DJ-41, trip to Djibouti |
| 29.6. | Measured stations DJ-42 and DJ-43 |
| 30.6. | --- --- DJ-44 - DJ-45 |
| 1.7. | Measuring equipment packed |
| 2.7. | Back to Djibouti and equipment shipped to Iceland |
| 3.7. | Meeting at ISERST and progress report submitted |
| 4.7. | Traveling from Djibouti to Iceland |
| 5.7. | ---- - --- - --- |

**Table 1.** Progress of field work.

The effective days for data acquisition were 25 and the total number of measured stations 45, giving an average of 1.8 stations per day. The locations of the measured stations are shown on Figure 1.

During the preparation of the project, a preliminary schedule and a station location plan was submitted to UNDP and ISERST. In this schedule the number of effective days for data collection had been estimated to be 24 and the expected performance estimated to be a minimum of 1 and a maximum of 2 soundings per day, resulting in minimum of 24 and maximum of 48 stations. The proposed station locations were placed on a rectangular grid, and the stations given different priorities. Highest priority was given to stations on a coarse grid covering the survey area. After preliminary interpretation of these stations the grid was to be condensed in order to fill in details in the emerging resistivity structure.

Because of difficult terrain and limited accessibility in the highly rifted prospect area, it was not possible to follow the proposed station location plan in details. At the end of each day a preliminary interpretation of data from the measured stations was performed in order to get a progressively clearer picture of the resistivity structure as the field work proceeded. After the highest priority stations had been measured, the station grid was condensed to fill in details.

When the prospect area in the central rift had been satisfactorily covered, a few days still remained of the field work time scheduled. This time was used to extend the station grid in a south-west direction, towards the area of the current drilling activity. This was done in order to enhance the connection of the results of the resistivity survey here reported with the results of a resistivity survey planned by Aquater in the latter area.

From the start of the field work until June 23, the field crew consisted only of the three Icelandic crew members instead of six people originally scheduled. The reason for this was that ISERST had trouble in providing English speaking field assistants. This made the field work more difficult than expected and slowed its progress in the beginning. After a few days, however, the field crew managed to attain the scheduled data acquisition rate to two stations per day. On June 23, ISERST provided one assistant, after which the field crew strength was brought up to four members.

The equipment used in this survey was EM37-3 unit from Geonics Ltd. in Canada. The technical aspects of the prospect method, instrumentation and data collection are briefly outlined in volume 2 of this report.

The electromagnetic noise level in the prospect area turned out to be very low so that the collected data is generally of a good quality and with a low noise level. An exception to this was station DJ-41, which had been placed near a seismic station and data transmitter in Lava Lake. The data from this station shows an anomalous behaviour compared to all the surrounding ones. This is probably due to electrical cables connected to the seismic transmitter disturbing the received signal in DJ-41. In addition some troubles were experienced in the synchronization between the TEM-transmitter and the TEM-receiver for this particular sounding. The sounding DJ-41 was therefore omitted in the interpretation.

## 3. DATA PROCESSING AND INVERSION

This section gives a brief discussion of the processing of the measured data and the inversion of the sounding results in terms of the resistivity structure. A more detailed discussion of these aspects can be found in volume 2 of this report.

In the TEM-method a loop of wire (transmitter loop) is placed on the ground and a magnetic field is built up by transmitting current into the loop. The current is abruptly turned off and the decay rate of the magnetic field measured by a receiver coil placed at the centre of the transmitter loop. The decay rate is dependent on and can be inverted in terms of the resistivity structure of the Earth under the transmitter loop.

The decay rate of the magnetic field, recorded as an induced voltage in the receiver coil, is stored in a data logger and later transferred to a personal computer for data processing and inversion.

The data processing consists of a renormalization of the recorded voltages to take into account the amplification in the receiver and a computation of a so called late-time apparent resistivity as a function of time after turn-off of the current in the transmitter loop. In section 5, volume 2, of this report there are listed the renormalized output voltages and the corresponding apparent resistivity values for all the measured soundings. The late-time apparent resistivity gives a convenient representation of the sounding results, but visual inspection of the apparent resistivity curves does not easily lend itself to giving detailed information about the subsurface resistivity structure. Hence a numerical inversion is needed.

The conversion of the apparent resistivity curves into resistivity models is done by one-dimensional inversion. In one-dimensional inversion it is assumed that the Earth can be divided into finite number of horizontal layers with constant and isotropic resistivity in each layer. By visual inspection of the data curve the number of layers and initial model parameters (the resistivity values and thicknesses of the layers) are estimated. The initial guess and the measured apparent resistivity values are loaded into an inversion program. The program computes the apparent resistivity curve corresponding to the guessed model. From the difference between the observed and calculated apparent resistivity values it iteratively adjusts the model parameters to find the model with the given number of layers that best fits the measured data. For each sounding an inversion was done with a different number of layers. Normally the model that fitted the data acceptably (with an average deviation of about 1 % between measured and calculated apparent resistivity values) with the fewest layers was taken to be the final model. In a few cases exceptions were made from this and a model with a higher number of layers selected in order to retain compatibility with adjacent soundings.

The one-dimensional inversion program used for the inversion of the present data is a nonlinear least square inversion program developed at Orkustofnun. The program uses an iterative inversion algorithm of the Levenberg-Marquart type along with a fast forward routine for computing the apparent resistivity response of a given model. The program can be run on both personal and main frame computers.

During the field work the collected data was loaded into a personal computer, processed and inverted. This was done in order to be able follow up the emerging resistivity structure of the prospect area so that the station grid could be made denser in strategic places where further details needed to be filled in.

After the team's return to Iceland, a final inversion of the data was performed at Orkustofnun. The one-dimensional resistivity models resulting from the inversion of the soundings were used to draw up resistivity cross-sections and maps. During interpretation of these sections and maps some of the soundings were reinverted in order to resolve ambiguities and inconsistencies in the sections.

The following general comments should be made on the one-dimensional inversion of the TEM-sounding data:

- The assumption that the resistivity structure is one-dimensional under each station is rather rough, and does in most cases, not hold true, but inversion of TEM-sounding data in terms of higher dimensional resistivity models is not jet commercially available. As discussed in volume 2, the loop-loop TEM-soundings are more downward focused and less sensitive to lateral resistivity variations than conventional direct-current soundings. Experience from Iceland has shown that one-dimensional inversion of loop-loop TEM-soundings can give almost the same resolution as a two-dimensional inversion of Schlumberger soundings. With this in mind it is considered acceptable to use one-dimensional inversion of loop-loop TEM-soundings except in cases of extreme lateral variations of resistivity.
- If the Earth beneath the sounding site is truly one-dimensional then there is theoretically a one to one correspondence between an observed, noise free apparent resistivity curve and the one-dimensional resistivity structure. But as soon as some noise is present in the data, slightly different models can give basically the same fit to the observed data and the result of the one-dimensional inversion becomes non-unique. Deviations from one-dimensionality of the actual resistivity structure has the same effect. This is a well known general problem in the inversion of resistivity data. A consequence of this is that the one-dimensional models have uncertainties. The degree of uncertainty in the model parameters is different, depending on the resistivity structure and the measured curve.

In the case of the models resulting from the inversion of the TEM-soundings in the Asal Rift, there is a great uncertainty is in the resistivity value of the uppermost high-resistivity layer, which is present in all the models. The same applies to the resistivity value of a resistive layer appearing underneath very low resistivity, which is present in nearly all the models. The presented resistivity values for these layers are probably in most cases in the lower part of a range of possible values. The resistivity of the top layer can probably be increased by a factor of two without greater influencing on the fit to the measured data. For the resistive basement layer it can likewise only be stated that its resistivity is higher than the resistivity of the layer above it.

The best determined model parameter is the depth down to the boundary where a high resistivity is underlain by a very low resistivity. This depth is determined to an accuracy of the order of 1 %. Other model parameters, resistivities and thicknesses of intermediate layers, are probably determined to an accuracy of about 20-30 %.

The inversions of the individual TEM-soundings need no special comments, except for station DJ-41. The model resulting from the inversion of this station showed an anomalous behaviour compared to the surrounding stations. This is probably, as mentioned in section 2, due to electrical cables connected to a seismic station and a data transmitter, disturbing the decaying magnetic field in the vicinity of the receiver coil in DJ-41. Because of this the model resulting from the inversion of the station DJ-41 was not used in the resistivity maps and sections.

The results of the inversion of all the 45 measured stations are shown in section 6, volume 2, of this report. The measured data points (small circles) are plotted as late-time apparent resistivity versus the square root of time after current turn-off (measured in microseconds). The one-dimensional resistivity model resulting from the inversion is shown both numerically as resistivities and thicknesses of the individual layers and also as a histogram where the x-axis shows the depth in meters and the y-axis the resistivity. The average fractional difference between the measured and calculated apparent resistivity values is also given as the quantity Chisq.

The resistivity models are listed in table 2. In this table two different models are found for a few of the stations. The two models have almost the same value of Chisq but different numbers of layers. These are the stations were exceptions were made by selecting the model with a greater number of layers in the interpretation.

# 4. INTERPRETATION OF THE DATA

In this chapter the results of the inverted data are interpreted. This is done by mapping the spatial distribution of the different resistivity layers and boundaries and correlating the resistivity structure to other physical parameters. Iso-resistivity maps and several resistivity cross sections are drawn, both across the Asal Rift and along it, and maps are made showing depth contours to various boundaries. From these maps and cross-sections conclusions are drawn as to the nature and extension of the geothermal activity by comparison with borehole data.

## 4.1 The layering of the resistivity

For almost all the soundings the best fit in the inversion of the data was obtained by using a model with four or five layers. Table 2 lists the result of the inversion in terms of the resistivities and the depth down to individual layers. When all the inverted soundings are compared, 6 different widespread layers of resistivity can be identified.

**Layer 1** is a high resistivity layer extending from the surface down to several tenths or a few hundreds of meters. It is found in all the soundings. The value of the resistivity in this layer is poorly defined since the dimensions of the soundings (loop size and recording time) were designed to give maximum resolution at greater depths. It can therefore only be stated that this is a layer of relatively high resistivity probably somewhere between a few hundred and a few thousand Ωm.

**Layer 2** has an intermediate resistivity somewhere in the range 10 to 50 Ωm, usually between 30 and 40 Ωm. It is only found in 15 of the 45 soundings. The actual value of the resistivity of this layer is poorly defined and can only be stated to be somewhere between 10 and 100 Ωm. The depth down to the top of this layer is not very accurate either. The inversion of most of the soundings was done both with and without considering this layer. In the case of the 15 soundings where this layer was kept in the final model the fit between the data and the model curve was considerably better. In the remaining 30 soundings the inversion program always made this layer very thin, and it could be removed without affecting the fit between the data and the model curve.

| Classification of layers | | | | Layer 1 | Layer 2 | | | Layer 3 | | | Layer 4 | | | Layer 5 | | | Higher resistivity beneath a low resistivity layer | | |
|---|---|---|---|---|---|---|---|---|---|---|---|---|---|---|---|---|---|---|---|
| Station number | Elevation (masl) | Num. of layers | Chisq. | $\rho_1$ (Ω m) | $\rho_2$ (Ω m) | $d_2$ (m) | $h_2$ (masl) | $\rho_3$ (Ω m) | $d_3$ (m) | $h_3$ (masl) | $\rho_4$ (Ω m) | $d_4$ (m) | $h_4$ (masl) | $\rho_5$ (Ω m) | $d_5$ (m) | $h_5$ (masl) | $\rho_6$ (Ω m) | $d_6$ (m) | $h_6$ (masl) |
| 1 | 110 | 4 | 0.011 | 176 | 12.8 | 138 | -28 | 3.9 | 226 | -116 | | | | 1.9 | 304 | -194 | 5.1 | 474 | -364 |
| 2 | 130 | 4 | 0.009 | 7390 | | | | 3.1 | 122 | 8 | 0.8 | 265 | -135 | 0.2 | 358 | -228 | | | |
| 3 | 120 | 3 | 0.011 | 12350 | | | | | | | 3.4 | 92 | 28 | 2.9 | 230 | -110 | | | |
| 4 | 120 | 4 | 0.009 | 920 | | | | | | | 1.5 | 124 | -4 | 12 | 171 | -51 | 3.5 | 291 | -171 |
| 5 | 85 | 4 | 0.008 | 2140 | | | | | | | 2.7 | 97 | -12 | 3.8 | 123 | -38 | 9.3 | 307 | -222 |
| 6 | 175 | 4 | 0.011 | 1975 | 36 | 66 | 109 | 7.0 | 178 | -3 | 2.7 | 226 | -51 | | | | | | |
| 7 | 80 | 3 | 0.009 | 530 | | | | | | | 3.0 | 207 | -127 | 1.6 | 297 | -217 | | | |
| 8 | 175 | 4 | 0.007 | 28250 | | | | | | | 3.9 | 276 | -101 | 9.2 | 373 | -198 | 4.1 | 457 | -282 |
| 9 | 275 | 9 | 0.007 | 846 | 10.3 | 249 | 26 | | | | 3.8 | 302 | -27 | | | | 56 | 601 | -326 |
| 10 | 280 | 4 | 0.009 | 816 | | | | 8.4 | 290 | -10 | | | | 1.9 | 354 | -74 | 52 | 535 | -255 |
| 11 | 200 | 3 | 0.019 | 258 | | | | | | | 2.3 | 234 | -34 | 1.3 | 276 | -76 | | | |
| 11 | 200 | 4 | 0.015 | 260 | | | | | | | 2.3 | 236 | -36 | 1.5 | 282 | -82 | 3.6 | 438 | -238 |
| 12 | 35 | 4 | 0.010 | 998 | | | | | | | 1.7 | 21 | 14 | 2.6 | 56 | -21 | 4.1 | 211 | -176 |
| 13 | 75 | 4 | 0.016 | 857 | 136 | 141 | -66 | | | | | | | 1.2 | 241 | -166 | 5.2 | 334 | -259 |
| 13 | 75 | 5 | 0.016 | 680 | 270 | 126 | -50 | 18.2 | 219 | -144 | | | | 1.1 | 242 | -167 | 4.8 | 329 | -253 |
| 14 | 180 | 4 | 0.009 | 1088 | | | | 7.1 | 286 | -106 | | | | 2.0 | 326 | -146 | 15.4 | 530 | -350 |
| 15 | 205 | 4 | 0.008 | 408 | 14.4 | 125 | 80 | 4.9 | 256 | -51 | | | | | | | 70.3 | 584 | -379 |
| 16 | 50 | 4 | 0.010 | 1550 | | | | | | | 2.0 | 58 | -8 | 3.4 | 91 | -41 | 17.4 | 308 | -258 |
| 16 | 50 | 5 | 0.010 | 2050 | 45.8 | 40 | 10 | | | | 2.0 | 59 | -9 | 3.4 | 90 | -40 | 18.8 | 310 | -260 |
| 17 | 115 | 4 | 0.011 | 1034 | | | | 5.5 | 264 | -149 | | | | 1.6 | 292 | -177 | 3.6 | 401 | -286 |
| 18 | 75 | 4 | 0.013 | 3226 | | | | | | | 0.9 | 224 | -149 | 2.0 | 264 | -189 | 9.6 | 389 | -314 |
| 19 | 90 | 5 | 0.011 | 931 | 48 | 58 | 32 | 4.5 | 191 | -101 | | | | 1.4 | 268 | -178 | 10.9 | 425 | -335 |
| 20 | 25 | 4 | 0.010 | 585 | | | | | | | 2.7 | 172 | -147 | 1.3 | 215 | -190 | 4.1 | 321 | -296 |
| 21 | 50 | 4 | 0.010 | 2095 | | | | | | | 1.5 | 47 | 3 | 1.9 | 67 | -17 | 8.3 | 184 | -134 |
| 22 | 120 | 4 | 0.007 | 991 | | | | 7.0 | 98 | 22 | 4.0 | 164 | -44 | | | | 6.8 | 392 | -272 |
| 23 | 110 | 4 | 0.015 | 539 | 30 | 68 | 42 | 4.5 | 157 | -47 | 2.3 | 262 | -152 | | | | | | |
| 23 | 110 | 5 | 0.013 | 491 | 31 | 68 | 42 | 4.6 | 157 | -47 | 2.5 | 261 | -151 | | | | 7.7 | 535 | -425 |
| 24 | 135 | 4 | 0.010 | 229 | 87 | 75 | 60 | 11.2 | 147 | -12 | 2.9 | 220 | -86 | | | | 21 | 635 | -500 |
| 25 | 125 | 4 | 0.009 | 422 | | | | 6.3 | 254 | -129 | | | | 1.5 | 304 | -179 | 13.9 | 484 | -359 |
| 25 | 125 | 5 | 0.009 | 453 | 39.0 | 220 | -95 | 4.9 | 266 | -140 | | | | 1.5 | 306 | -180 | 14.0 | 482 | -360 |

**Table 2.** Results of the inversion of the TEM-soundings. $\rho_i$ denotes the resistivity of the i'th layer, $d_i$ and $h_i$ denote the depth and the elevation of the top of the i'th layer. The average fractional difference between the measuered and calculated resistivity values is denoted by Chisq.

| Classification of layers | | | | Layer 1 | Layer 2 | | | Layer 3 | | | Layer 4 | | | Layer 5 | | | Higher resistivity beneath a low resistivity layer | | |
|---|---|---|---|---|---|---|---|---|---|---|---|---|---|---|---|---|---|---|---|
| Station number | Elevation (masl) | Num. of layers | Chisq. | $\rho_1$ (Ω m) | $\rho_2$ (Ω m) | $d_2$ (m) | $h_2$ (masl) | $\rho_3$ (Ω m) | $d_3$ (m) | $h_3$ (masl) | $\rho_4$ (Ω m) | $d_4$ (m) | $h_4$ (masl) | $\rho_5$ (Ω m) | $d_5$ (m) | $h_5$ (masl) | $\rho_6$ (Ω m) | $d_6$ (m) | $h_6$ (masl) |
| 26 | 240 | 4 | 0.012 | 649 | 38 | 196 | 44 | 3.9 | 246 | -6 | | | | | | | 9.9 | 428 | -188 |
| 27 | 200 | 4 | 0.012 | 1270 | | | | 7.5 | 321 | -121 | | | | 1.7 | 378 | -178 | 14 | 568 | -368 |
| 28 | 70 | 5 | 0.008 | 380 | 23 | 88 | -18 | | | | 3.7 | 183 | -113 | 1.2 | 245 | -175 | 15.2 | 394 | -324 |
| 29 | 75 | 4 | 0.013 | 1660 | | | | | | | 1.9 | 67 | 8 | 3.1 | 97 | -22 | 6.9 | 293 | -218 |
| 30 | 85 | 3 | 0.010 | 840 | | | | | | | 2.3 | 72 | 13 | | | | 16.7 | 278 | -193 |
| 31 | 115 | 4 | 0.008 | 243 | | | | 2.2 | 125 | -10 | 4.3 | 178 | -63 | 2.9 | 317 | -202 | | | |
| 32 | 260 | 4 | 0.016 | 850 | | | | 9.1 | 270 | -10 | 2.9 | 368 | -108 | | | | 20.2 | 644 | -384 |
| 33 | 130 | 5 | 0.008 | 3590 | | | | 2.6 | 122 | -8 | 7.0 | 169 | -69 | 3.0 | 218 | -88 | 35 | 436 | -306 |
| 34 | 115 | 4 | 0.009 | 857 | | | | | | | 3.5 | 113 | 2 | 5.6 | 185 | -70 | 3.6 | 325 | -210 |
| 35 | 25 | 4 | 0.009 | 1080 | | | | | | | 2.5 | 125 | -100 | 0.9 | 160 | -135 | 2.9 | 260 | -235 |
| 36 | 240 | 4 | 0.007 | 1440 | | | | 7.7 | 239 | 1 | 2.8 | 339 | -99 | | | | 8.7 | 520 | -280 |
| 37 | 105 | 5 | 0.014 | 2200 | 349 | 227 | -122 | | | | 0.9 | 268 | -163 | 1.5 | 308 | -203 | 10.9 | 426 | -321 |
| 38 | 210 | 5 | 0.006 | 398 | 24.0 | 192 | 18 | | | | 2.5 | 238 | -28 | 1.3 | 290 | -80 | 5.0 | 472 | -262 |
| 39 | 225 | 4 | 0.012 | 1546 | 362 | 304 | -79 | | | | | | | 1.3 | 335 | -110 | 2.4 | 350 | -125 |
| 39 | 225 | 5 | 0.009 | 1588 | 331 | 300 | -75 | | | | 1.5 | 338 | -112 | 2.7 | 356 | -130 | 7.9 | 611 | -385 |
| 40 | 205 | 4 | 0.010 | 701 | | | | | | | 1.5 | 261 | -56 | 2.2 | 294 | -89 | 6.4 | 507 | -302 |
| 41 | 115 | 5 | 0.009 | 1618 | 36.4 | 65 | 55 | | | | 3.8 | 107 | 8 | 1.3 | 241 | -126 | 4.3 | 268 | -154 |
| 42 | 240 | 4 | 0.009 | 526 | 15 | 196 | 44 | | | | 2.9 | 300 | -160 | | | | 17.4 | 520 | -280 |
| 42 | 240 | 5 | 0.007 | 631 | 16.7 | 191 | 49 | 4.5 | 284 | -44 | 2.6 | 327 | -87 | | | | 9.9 | 483 | -243 |
| 43 | 140 | 4 | 0.005 | 56.7 | | | | 7.2 | 57 | 83 | 4.2 | 132 | 8 | 1.1 | 280 | -140 | | | |
| 44 | 200 | 4 | 0.008 | 50.8 | | | | 2.2 | 52.3 | 148 | 1.1 | 102.2 | 97.8 | 3.0 | 118.2 | 81.8 | 9.6 | 429 | -229 |
| 45 | 200 | 5 | 0.008 | 124 | | | | 2.8 | 79 | 121 | 1.4 | 123 | 77 | 1.1 | 157 | 43 | 44 | 293 | -93 |

**Table 2** (continued)

Figure 2 is a map showing the extent and thickness of layer 2 (the thickness is zero where the layer is absent) and Fig. 3 shows a three dimensional picture of the same. It is interesting to see how this layer seems to exist only along a transverse belt crossing the central rift zone from north to south just west of Lava Lake. It is also tempting to conclude from Fig. 3 that the thickness of this layer is greatest over some of the main faults in the rift zone.

**Layer 3** is characterized by resistivity values in the range 4 to 10 Ωm and is underlain by a layer of still lower resistivity. It is only found in a part of the prospect area. Figure 4 shows the thickness and extent of this layer. By comparison of Figs. 2 and 4 it can be concluded that the extent of layers 2 and 3 is very similar, these layers appear as a belt crossing the rift just west of Lava Lake. The depth down to layer 3 is one of the best defined parameters in the inversion, determined to an accuracy of a few meters. Its resistivity value is not as well determined.

**Layer 4** is a low-resistivity layer and exists in all of the soundings. The value of the resistivity is usually 1 to 4 Ωm with one exception where its value is considerably lower than 1 Ωm (DJ-02). The depth to the top of this layer is very well defined especially where layer three is absent. The uncertainty in this depth estimate is only few meters. The value of the resistivity is probably determined with 20-30% uncertainty.

**Layer 5** is found in some of the measurements and has a slightly different resistivity value from that of layer 4, in some cases a little higher and in others a little lower. It is in most cases rather poorly defined, both in terms of the resistivity value and the boundary to layer 4. It is, however, necessary to include it in the inversion to obtain an acceptable fit to the data.

Fig. 5 shows a contour map of the lowest resistivity values found in layers 4 and 5. On this map it is striking out that the value of the resistivity in these layers is generally higher on a belt crossing the central rift zone near Lava Lake.

**Layer 6** is a high-resistivity layer. The value of the resistivity in this layer is very poorly defined and can in most cases only be stated to be somewhat higher than that in the overlying layer. Figure 6 shows the upper boundary of this layer. Even though the uncertainty expected in the calculated depth down to layer 6 is rather large, the figure shows a very consistent picture. There is a systematic increase in depth of layer 6 towards Lava Lake, where it is either absent or below the depth of penetration of the TEM-soundings.

## 4.2 Cross sections

A total of twelve resistivity cross-sections were drawn. The locations of these are shown on Figure 7. The cross sections are divided into two groups, one includes the cross-sections perpendicular to the rift zone (sections GG', HH', II', JJ', KK' and LL') and the other includes the cross-sections along the rift (sections AA', BB', CC', DD', EE' and FF').

**Cross-sections along the Asal Rift** are shown on Figures 8 - 13. From these sections the following features are obvious:

- All the sections show a sudden change in the upper boundaries of layers 3 and 4 in such a way that the depth to these boundaries increases considerably towards west over a short distance just west of Lava Lake.
- The high-resistivity layer at depth (layer 6) is absent in and around Lava Lake in sections BB', CC' and DD'.
- The resistivity value of the low-resistivity layers generally decreases towards Lake Asal.
- The resistivity structure below Lava Lake is more complicated than elsewhere (sections BB' and JJ').
- The existence of layer 2 seems to be restricted to the area where layers 3 and 4 are dipping steeply down.
- The top of resistivity layers 2 and 3 and in some cases of layer 4 is found to be above sea-level in the eastern part of the area in sections passing through Lava Lake.

**Cross-sections across the Asal Rift** are shown on Figures 14-19. Following information can be extracted from these sections:

- The resistivity layers are displaced by approximately 150 m in the southern part of the surveyed area. The soundings DJ-11, DJ-38 and DJ-40 are north of the fault but soundings DJ-43, DJ-44 and DJ-45 are south of it. This displacement seems to coincide with a fault zone between boreholes Asal 4 and Asal 3. The displacement of the resistivity layers across the fault is similar to that observed comparing the lithological logs of these two boreholes.
- With the exception of these southernmost faults there is no obvious correlation between the displacements of the resistivity layers and the faults.
- Sections GG', KK' and FF' indicate updoming of layer 2 in the vicinity of the faults near Lava Lake.
- Under Lava Lake the high-resistivity layer (layer 6) is absent or below the depth of penetration of the TEM soundings.
- The resistivity structure is more complicated in and around Lava Lake than elsewhere.

## 4.3 The physical meaning of the resistivity layers

### 4.3.1 General comments on the dependence of resistivity on other parameters

The resistivity of the upper crust depends on several parameters. The resistivity structure of pure basaltic crust has been investigated in Iceland and since the crust in the Asal Rift is quite similar to the rift zones of Iceland the experience from Iceland might apply to the Asal Rift in Djibouti.

The resistivity value depends on the following factors:

1. **Degree of water saturation**
   Above the water table the resistivity value of unaltered basaltic lavas in Iceland is of the order of $10^4$ Ωm. Below the water table its value drops to the order of $10^3$ Ωm in case of fresh water but to the order of 10 Ωm when saturated with cold sea-water.

2. **The stage of the alteration of the rock**
   In the argillic zone the clay minerals form a thin conducting film on the surface of the pores and fractures, causing the resistivity value to drop down to 40-50 Ωm (fresh water saturation) compared to the value of $10^3$ Ω in the freshwater saturated unaltered zone. In this case the conduction of an electrical current takes place along the clay film on the pore walls (interface conduction) rather than by ionic conduction in the pore fluid. If the pore fluid, however, has very high salinity (sea-water) the ionic conduction becomes more important than the interface conduction. The top of the argillic zone can therefore form a boundary between resistivity layers, but only when the resistivity of the pore fluid is rather high (>5 Ωm at 25°C). In the phyllic zone the alteration minerals are less conductive than in the argillic zone due to a different crystal structure. In low salinity geothermal systems this can lead to an observable increase in the formation resistivity at the transition from the argillic to the phyllic zone.

3. **Porosity of the rock**
   Resistivity decreases with increasing porosity of the rock formation. This is the case for both ionic and interface conduction. This causes resistivity to be relatively higher in areas of strong secondary mineralization where the secondary minerals fill the pores. For example precipitation of anhydrite or calcite could lead to increased resistivity. In areas of intense fracturing porosity can be expected to increase causing reduction in resistivity.

4. **Formation temperature**
   Resistivity is highly dependent on temperature both in the case of ionic and interface conduction and decreases with increasing temperature. For ionic conduction and partly in the case of interface conduction equations have been established connecting the formation temperature and the bulk resistivity of rocks.

5. **Salinity of the pore fluid**
   In the unaltered zone and the phyllic zone (no interface conduction) and in sea-water saturated rock, the bulk resistivity of the rock is proportional to the pore fluid resistivity according to Archie's law. The pore fluid resistivity is almost inversely proportional to the concentration of dissolved ions and can be calculated from the chemical content of the fluid.

6. **Boiling**
   Where the formation temperature reaches the boiling point at the ambient pressure a sudden increase in resistivity occurs since the pores are now partially filled with steam instead of water.

In addition to the above listed factors affecting resistivity, experience from

investigating high temperature geothermal fields in Iceland has shown that:

- there is no general correlation between lithology and resistivity. Layers of different resistivity do not correspond in general to distinct lithological units. The resistivity layers are primarily layers of certain physical state such as temperature, porosity, etc. Occasionally these resistivity layers may coincide with certain lithological units but in general they do not.
- in brine dominated geothermal systems the interface conduction is of little importance. It follows that the disappearance of interface conduction in passing through the boundary between the argillic and the phyllic zone is not to be observed in such geothermal systems.

All the above mentioned factors must be kept in mind when interpreting a resistivity survey like the one carried out in the Asal Rift. Because of the number of parameters which can affect the resistivity structure it is almost impossible to make sensible conclusions about the physical and geological meaning of the resistivity structure by looking only at the results from the soundings. However, by making use of other available geological and geophysical data from the research area (especially boreholes) and the experience from surveys in geologically similar environments (in this case Iceland) the results of the TEM-soundings can be used to make a conceptual model of the geothermal system.

### 4.3.2 The data from the boreholes

Six boreholes have been drilled within the area of investigation. On the maps they are marked A-1 to A-6, whereas on the cross sections they are referred to as Asal-1 to Asal-6. Three of these wells, A-1, A-3 and A-6, are quite close to each other. The cross-sections GG', JJ', LL', DD' and CC' are close to some of the boreholes and information from these wells has been projected onto the cross-sections. The information is taken from reports made by Aquater. The borehole data used for comparison include:

- Lithological structure obtained from analysis of drill cuttings
- Alteration zoning obtained from secondary minerals
- Information on the water table in the uncased well
- Measurements of formation temperature

**Asal 4** is close to the sounding DJ-11. The following has been observed comparing this borehole and the sounding:

1. The water table and the top of the argillic zone is found exactly at the boundary between layer 1 and an underlying layer (layer 4) having a resistivity value of 2.3 Ωm
2. The boundary between layer 4 (2.3 Ωm) and layer 5 (1.9 Ωm) is close to the boundary between basaltic and hyaloclastic units in the well.

3. The boundary between layer 5 and the underlying layer (layer 6) is about 30 m below the bottom of the hyaloclastite formation where basalt and scoria are found.
4. The temperature in layer 4 (2.3 Ωm) is somewhat lower than 50°C.
5. There is a continuous and a considerable increase in the temperature from 50°C in the upper part of layer 5 and down through the boundary between layer 5 and layer 6.
6. The top of the phyllic zone is about 100 m below the boundary between layers 5 and 6.

From this comparison the following conclusions can be drawn:

- The high-resistivity surface layer (layer 1) correlates with a basaltic lava pile above the water table.
- The boundary between layer 1 and layer 4 charts the water table, at least when the layers 2 and 3 is missing.
- The very low resistivity values below the water table indicates pore fluid of high salinity (brine saturation).
- The boundary between layers 4 and 5 could either reflect higher porosity in the hyaloclastite than in the overlying basalts or increasing salinity with depth.
- The boundary between layers 5 and 6 is likely to be caused by increasing secondary mineralization (top of phyllic zone) causing reduction in the porosity.

**Asal 5** is located in Fieale in the central rift west of Lava Lake. It is close to sounding DJ-01. The following can be deduced from comparison between the borehole data and the sounding:

1. The lithology consist of a sequence of basalts and trachytes. The unaltered zone extends down to approximately 300 m below sea level where the argillic zone starts. From this it is evident that the nature of the resistivity boundaries are not lithological.
2. The water table is found at approximately 200 m depth below the wellhead. This is close to the boundary between layers 2 and 3 which means that the top of layer 3 marks the water table where that layer is present.
3. There are no signs of any change in lithology or mineralogy between layers 3 and 4 but the lowering of the resistivity in layer 4 might be due to continuously increasing temperature or salinity with depth.
4. The boundary between layer 4 and layer 6 (the high resistivity layer) is close to the depth where the temperature starts decreasing with depth, but it is also not far away from the top of the phyllic zone. It is rather unlikely that the increase in resistivity can be attributed to decreasing temperature with depth because the temperature inversion only becomes important at about 200m below the observed increase in the resistivity. The most likely explanation is a pronounced

decrease in the porosity at this depth which in fact is consistent with the rather sharp increase in type and intensity of the alteration observed in Asal 5.

The analysis of drill cuttings from Asal-5 showed non-equilibrium between the current temperature and the alteration minerals, indicating much higher temperatures than are found at present. The sharp top in the temperature-depth curve at approximately 300 to 400 m.b.s.l. is more likely to be caused by intersection with a permeable and dipping fault zone rather than a widespread inversion of temperature with depth.

**Asal 1 and 3** are approximately 1 km away from the nearest sounding (DJ-45) and hence the comparison between the borehole data and the sounding is rather doubtful. The following should, however, be noted:

1. In these wells the top of the argillic zone is just about 20 m below the wellhead and within resistivity layer 1. This indicates that the lower boundary of layer 1 has nothing to do with the top of the argillic zone.
2. The free water level in Asal 1 and 3 is not well known to us, but the information we have indicates a water table close to sea level. This is completely in disagreement with the results of the TEM-soundings which give a resistivity value of 2.8 Ωm at approximately 80 m depth. It is impossible to have such a low resistivity without water saturation so it is concluded that the water table around wells No. 1,3 and 6 must be close to that depth. This water level could be a false water table due to impermeable horizontal layers.
3. Below the 2.8 Ωm layer the resistivity decreases to 1.1 Ωm. Over the same depth interval the temperature observed in the boreholes is only increasing very slowly and no change observed in lithology or secondary minerals. Increasing salinity or porosity with depth might explain this reduction in resistivity.
4. A high-resistivity layer is observed at 90 m.b.s.l. It could be related to boundary between basalt scoria and claystone or imply the top of the phyllic zone (reduced porosity).

**Asal-2** is close to sounding DJ-44. Unfortunately, the information we have from this well is rather sparse, consisting only of information about its lithology and temperature. Following items should be noted:

1. The lower boundary of layer 1 (the water table) is approximately at 50 m depth.
2. There is no resistivity boundary seen near the transition from basalt to hyaloclastite.

### 4.3.3 Conclusions on the nature of resistivity boundaries in the Asal Rift

On basis of the comparison between the resistivity structure and the borehole data, the following conclusions are made about the nature of the resistivity layers in the Asal Rift.

1. The geological interpretation of the uppermost high-resistivity layer (layer 1) is that it consists of volcanic rock of basaltic origin but above water table. The value of the resistivity in this layer is in general lower than that expected from

comparison with similar data from Iceland, but it should be kept in mind that this value is poorly defined.

2. The sudden change in resistivity at the bottom of layer 1 coincides with the water table, at least where layer 2 is absent. In soundings where layer 2 is present it is possible that the boundary between layer 2 and layer 3 gives the water table. In that case the physical meaning of layer 2 would be an area of partially saturated rocks caused by condensation of updraughting steam.
3. Layer 3 is basaltic and lies below the water table. The boundary between layers 3 and 4 is likely to reflect different salinity of the pore fluid, i.e. the salinity of the pore fluid in layer 3 could be somewhat less than that of sea-water.
4. Layers 4 and 5 are sea-water saturated basalts within the argillic zone. The difference between these layers is probably due to a change in salinity and/or porosity with depth.
5. The variation in resistivity within layer 4 (0.8-4 Ωm) from one place to another is considered to be due to the effects of different salinity, temperature and porosity.
6. The relatively high resistivity in layer 6 is considered to be due to increasing secondary mineralization which fills the pores and thus reduces the porosity. The reasons for this conclusion are:
   - Layer 6 appears in most cases close to the top of the phyllic zone in the boreholes.
   - There is except close to Asal-5 a continuous increase in temperature from layers 4 and 5 and into layer 6, which should cause decreasing resistivity with depth.
   - Decrease in salinity with depth is unlikely and in direct contradiction with the results of chemical analysis (Asal-3).
   - Boiling can be ruled out on basis of measured temperature.
   - Change in conduction mechanism is also an unlikely explanation since ionic conduction is considered to be dominant in the argillic zone where the pores are saturated with sea-water

Reduction in porosity is therefore the only possible parameter to cause observed increasing resistivity with depth. A consequence of this is that the absence of layer 6 below Lava Lake is most likely due to a temperature anomaly, i.e. the increase in temperature with depth is so rapid that it counteracts the effect of reduction in porosity.

## 4.4 The water table

One of the most interesting information obtained by the TEM-survey is the mapping of the water table. In the discussions above it was concluded from comparison between the borehole data and the TEM-data that the water table is represented by

the surface of layer 3 (4-10 Ωm), or the surface of layer 4 (< 4 Ωm) where layer 3 is missing. Both of these surfaces are determined by the TEM-soundings with very good accuracy. Figure 20 shows a map of this surface, i.e. the water table. On this map several very interesting features are clearly to be seen:

- There is a strong gradient evident in the elevation of the water table traversing the central rift between the borehole Asal 5 and Lava Lake. East of this gradient the water table is close to sea level but west of it the water table is close to the surface of Lake Asal. This indicates strongly a hydrological barrier (low permeability zone) crossing the central Asal Rift just west of Lava Lake.
- Close to sounding DJ-02 an irregularity comes to light in the transverse step in the elevation of the water table probably caused by a tectonic breakup of the barrier at some time.
- East of this barrier the water level is found to be above the sea level with maximum elevation in and around Lava Lake. This is concluded to indicate a geothermal upflow zone. This conclusion is strongly supported by the distribution of fumaroles.
- There is a sudden increase in the elevation of the water table towards southwest across the main fault between Asal-4 and Asal-3. The fault itself might act as a hydrological barrier. It is possible that the water table southwest of the fault is false.

## 4.5 Isoresistivity maps

On Figures 21-25 isoresistivity maps have been drawn to give the resistivity values at sea level, at 100, 200, 300 and 400 m depth below sea level. This is just an alternative presentation of the data. They give the same information as that deduced from the previous maps and cross-sections but some of the features are easier to see on the isoresistivity maps.

The map of the resistivity at sea level displays very clearly the areas where the water table is above sea level i.e. the areas where the resistivity is below 8 Ωm. This is the case in Lava Lake and east of it and also south of the main fault between wells Asal-4 and Asal-3.

The map of the resistivity values at 100, 200 and 300 m below sea level show clearly the transverse barrier crossing the rift close to Asal-5. They display the very low resistivity in the neighbourhood of the wells Nos. 1,2,3,4 and 6 as well as in the area close to Lake Asal. This resistivity low is interpreted as a sign of ultra high salinity.

The map of the resistivity at 400 m below sea level shows the absence of layer 6 (high resistivity ) below Lava Lake, an indication of higher temperatures in this region than elsewhere at similar depth.

# 5. CONCLUSIONS AND A MODEL OF THE GEOTHERMAL ACTIVITY IN THE CENTRAL ASAL RIFT

The main results of the TEM-survey can be summarized as follows:

1. Six different widespread resistivity layers are identified in the uppermost 700 m of the crust in the Asal Rift. The physical meaning of each of them is:
   - Layer 1 consists of rock of basaltic origin above the water table.
   - Layer 2 is primarily found to exist where there is a rapid change in the water level around Lava Lake. This layer is interpreted as a partially water-saturated zone probably due to condensation of steam emerging from greater depths.
   - Layer 3 comprises water saturated rock. The salinity of this layer is probably lower than of the underlying layers. The top of it marks the groundwater table.
   - Layer 4 consists of sea-water saturated rock. In the case where layer 3 is absent the top of this layer denotes the groundwater table.
   - Layer 5 is not present everywhere but is interpreted as a layer with different salinity or porosity than in layer 4.
   - Layer 6 represents considerable reduction in porosity due to secondary mineralization. Its top coincides roughly with the top of the phyllic zone.
2. An impermeable zone (a hydrological barrier) crosses the central Asal Rift between well Asal-5 and Lava Lake. This is reflected by a sudden drop in the water table towards Lake Asal.
3. The fault between wells Asal-4 and Asal-3 is also a hydrological barrier separating the water table in the central rift from higher water levels caused by the mountainous area south of the Rift zone.
4. The high resistivity layer (layer 6) is not observed below the Lava Lake. This is interpreted as an indication of considerably higher temperatures below the Lava Lake than elsewhere at a similar depth in the surveyed area.
5. The increased resistivity in layers 4 and 5 in the area around Lava Lake is either due to reduced porosity caused by secondary mineralization or due to lower salinity than elsewhere or a combination of both.
6. Sounding number DJ-02 close to Lava Lake shows extremely low resistivity all the way from the water table down to the maximum depth of penetration of this sounding (about 600 m). This is an indication of high temperature in relation to the surroundings.
7. The indication that layer 2 rises up to shallower depths along some of the main faults of the central rift implies that the faults are permeable.

On the basis of the conclusions above, the general knowledge of the geology of the Asal Rift and the experience gained from investigations on high temperature geothermal fields in the rift zones in Iceland, the following model is proposed for the geothermal activity in the central Asal Rift.

In the area between Ghoubbet al Kharab and Lake Asal there is a general underground flow of sea-water towards Lake Asal along the rift zone driven by the pressure difference between the sea level and the level of Lake Asal (150 m.b.s.l.)

Below Lava Lake this general flow is interrupted by local upflow of geothermal fluid, mainly along open fissures connected to the active faults. This upflow creates an anomaly in the water level causing it to rise above the sea level. From this it follows that there must be a local anomaly in the direction of the general groundwater flow from the upflow zone in Lava Lake towards the sea.

The conclusion of an upflow zone in Lava Lake is further supported by the presence and the distribution of fumaroles and the absence of high resistivity at depth.

The impermeable zone just west of Lava Lake is either of tectonic origin, or which is more likely, created by precipitation of secondary minerals (such as calcite) from cooling geothermal fluid. There is a big pressure drop across this zone. Hot water which migrates through the barrier along fractures is likely to flash due to the pressure release causing precipitation of secondary minerals which cause the barrier to build up sealing off the upflow zone. Due to the boiling the salinity of the fluid passing through the barrier is increased. Furthermore the steam from the flashing of water penetrating the barrier will move upwards, condense and create the partially saturated layer 2.

Above the upflow zone there will also be precipitation of secondary minerals from the ascending geothermal fluid which has in a period of hundreds or thousands of years caused reduced porosity of the rock. This is reflected by relatively higher resistivity at shallow depth in the upflow zone. As a consequence of this the primary porosity and hence the general permeability of the basaltic lava pile in the upflow zone can be expected to be rather low compared to the surroundings.

On the other hand the rift zone is tectonically active so that secondary porosity caused by formation of faults and fissures can be expected to be high. Therefore productive aquifers are primarily expected along active faults or fissures. The distribution of the fumaroles along the faults supports this theory.

At last the following explanation is suggested for the observed nonequilibrium between the alteration and the present temperature in Asal-5:

In the geologically recent past, perhaps until approximately 200,000 years ago the main activity in the Asal Rift was associated with volcanic axis that do not necessarily coincide with the present axis. One of those is represented by the hyaloclastite formations in the vicinity of Asal-1,2 and 3. The fossil alteration in the present rift as revealed by Asal-5 was then already created and the top of the argillic zone was at that time close to the surface like in Asal 1-3. When the present rift opened up with intense fracturing, the area affected cooled down due to flow of cold water (during

pluvials) or sea-water (during interpluvials) along these fractures between Ghoubbet al Kharab and Lake Asal. In addition the area subsided and new basaltic lava was formed on the surface, which represented by uppermost unaltered rocks in Asal-5.

As time passed the volcanic activity reaching its maximum at Lava Lake led to a formation of a convective geothermal system probably in response to a localized concentration of intrusions. The upflow part of the system is below Lava Lake and a self sealing processes caused by precipitation from cooling geothermal fluid has created a hydrological barrier around the upflow zone. Crustal movements due to rifting episodes cause the barrier to break up along some of the faults and some geothermal fluid to escape. The maximum value of the temperature at 500 m depth in Asal-5 is considered to be due to such leakage along a fault through the barrier.

## 6. RECOMMENDATIONS

In view of the result of the TEM-survey and with regard to our experience from exploring and exploiting geothermal fields in Iceland similar to those in the Asal Rift it is recommended to drill an exploratory well in the proposed upflow zone of the geothermal field in Lava Lake. It should preferably not be shallower than 800 meters to ensure that it penetrates into the depth range where high resistivity is observered to be absent.

From our data, the two preferred sites for the borehole within the area of interest, are near sounding DJ-02 and near sounding DJ-03.

By siting the first exploratory well close to DJ-02 it will be drilled where the lowest resistivity within the upflow zone is observed. If this very low resistivity is due to a temperature anomaly this is likely to be the most interesting place to drill.

On the other hand by siting the borehole near DJ-03 it will be close to the fumaroles which are a guide to an underlying geothermal system. There are no fumaroles in the vicinity of DJ-02. Therefore it is preferable to drill the first exploratory well close to sounding DJ-03.

In both cases the drill site should be selected so that the borehole intersects a nearby tectonic fracture or fault i.e. should be located at such a distance from the fault or fracture that the hole will cut through it within a certain depth range. It is especially important that a borehole near DJ-03 intersects the faults which the fumaroles are connected to.

# 7. SOURCES OF INFORMATION

In the interpretation of the TEM-data and subsequent conceptual modeling of the geothermal activity a lot of information from other sources is used. It is not referred directly to the sources of information in the text but they are however the basis for the conclusions drawn in this report. These include:

1. General information on the geology of the Asal Rift as well as results from geothermal prospecting and drilling in the area.
   - Asal 4 Well Report. A report prepared by Aquater Eni Group, March 1988.
   - Asal 5 Well Report. A report prepared by Aquater Eni Group, April 1988.
   - Copies of summaries of the results from drilling of wells 1-6 prepared by Aquater.
   - A.Gerard, C.Mennechet, P.Puvilland, 1980: Champ Géothermique D'Asal. Syntése des données disponibles au 1er Juin 1980. A BRGM report.
   - A. Abdallah, A. Gerard, J. Varet, 1982: Construction d'un Modéle synthétique du Champ Géothermique D'Asal. A BRGM report.
   - V. Barthes, A Gerard, J.Varet, 1980: Champ Geothermique D'Asal. Syntése des données disponibles. A BRGM report.
   - V. Barthes and A. Gerard, 1980: Traitement des données aeromagnétiques en République de Djibouti region Ghoubbet - Asal. A BRGM report
   - Geological Map of the Asal Rift, prepared by BRGM.
   - Kristján Saemundsson, 1988: Djibouti Geothermal Project. Analysis of geological data pertaining to the geothermal exploration of the Asal Rift.
2. Papers and reports describing exploration and exploitation of high temperature geothermal fields in Iceland where the geological situation is quite similar to the Asal Rift.
   - Knútur Árnason, Ólafur G. Flóvenz, Lúðvík S. Georgsson and Gylfi Páll Hersir, 1987: Resistivity Structure of High Temperature Geothermal Systems in Iceland. IUGG XIX General Assembly, Vancouver Canada, August 9-22, 1987. Abstracts V.2: 447.
   - Knútur Árnason et al. 1987: Nesjavellir-Ölkelduháls. A report from Orkustofnun on geophysical an geological investigation of the Nesjavellir high temperature field in SW-Iceland (In Icelandic with English summary). OS-87018/JHD-02.
   - Ólafur G. Flóvenz, Lúðvík S. Georgsson and Knútur Árnason, 1985: Resistivity Structure of the Upper Crust in Iceland. Journal of Geophysical Res. vol. 90 pp 10136-10150.
   - Lúðvík S. Georgsson, 1981: A Resistivity Survey on the Plate boundaries in the Western Reykjanes Peninsula, Iceland. Geothermal Res. Council,

Transactions, vol. 5, October 1981.

- Lúðvík S. Georgsson, 1984: Resistivity and Temperature Distribution of the Outer Reykjanes Peninsula, Southwest Iceland. 54th Annual International SEG Meeting, December 2-6, 1984 Atlanta, Georgia. Expanded Abstracts, pp 81-84.

# FIGURES

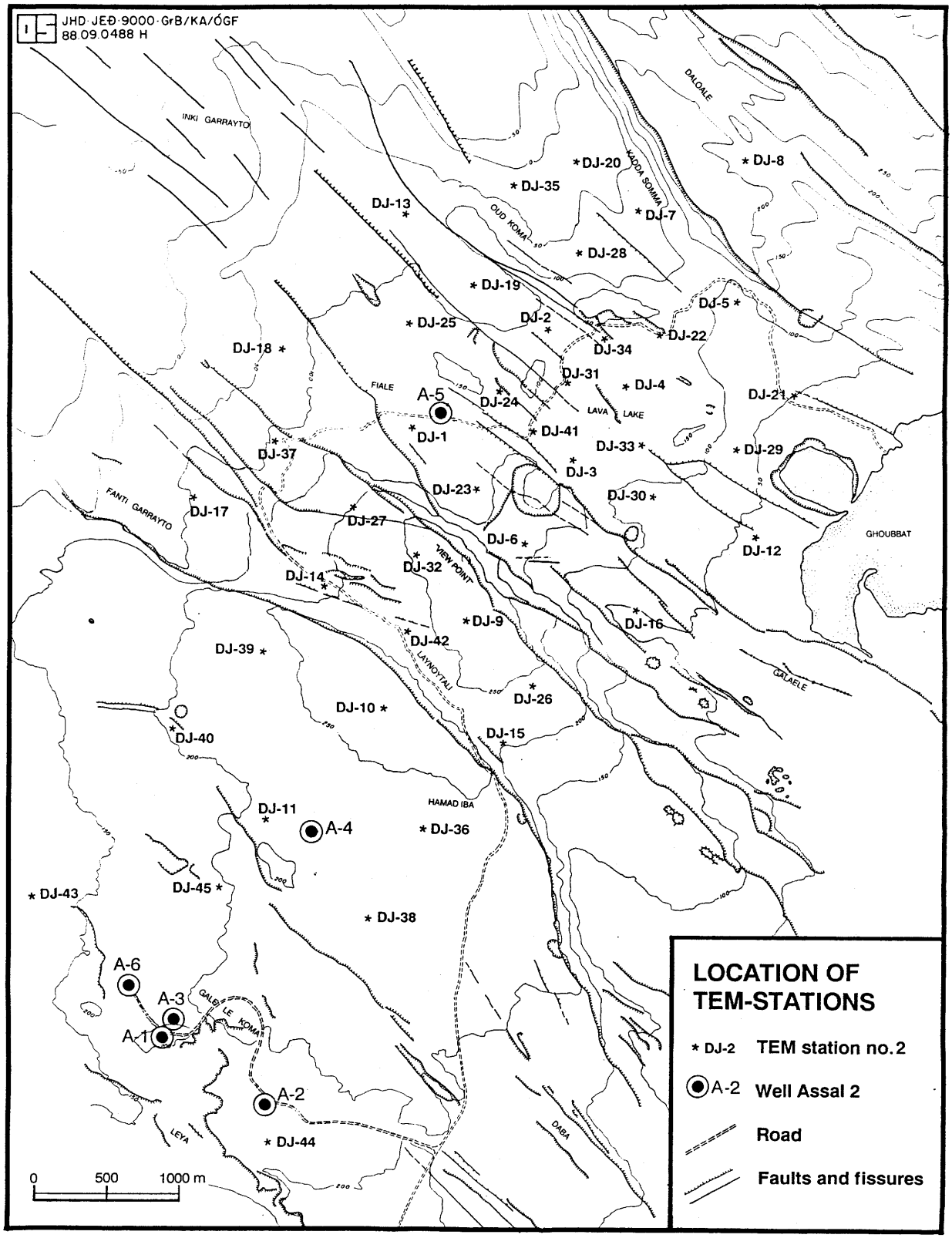


**Figure 1.** The location of TEM-soundings in the Asal Rift.

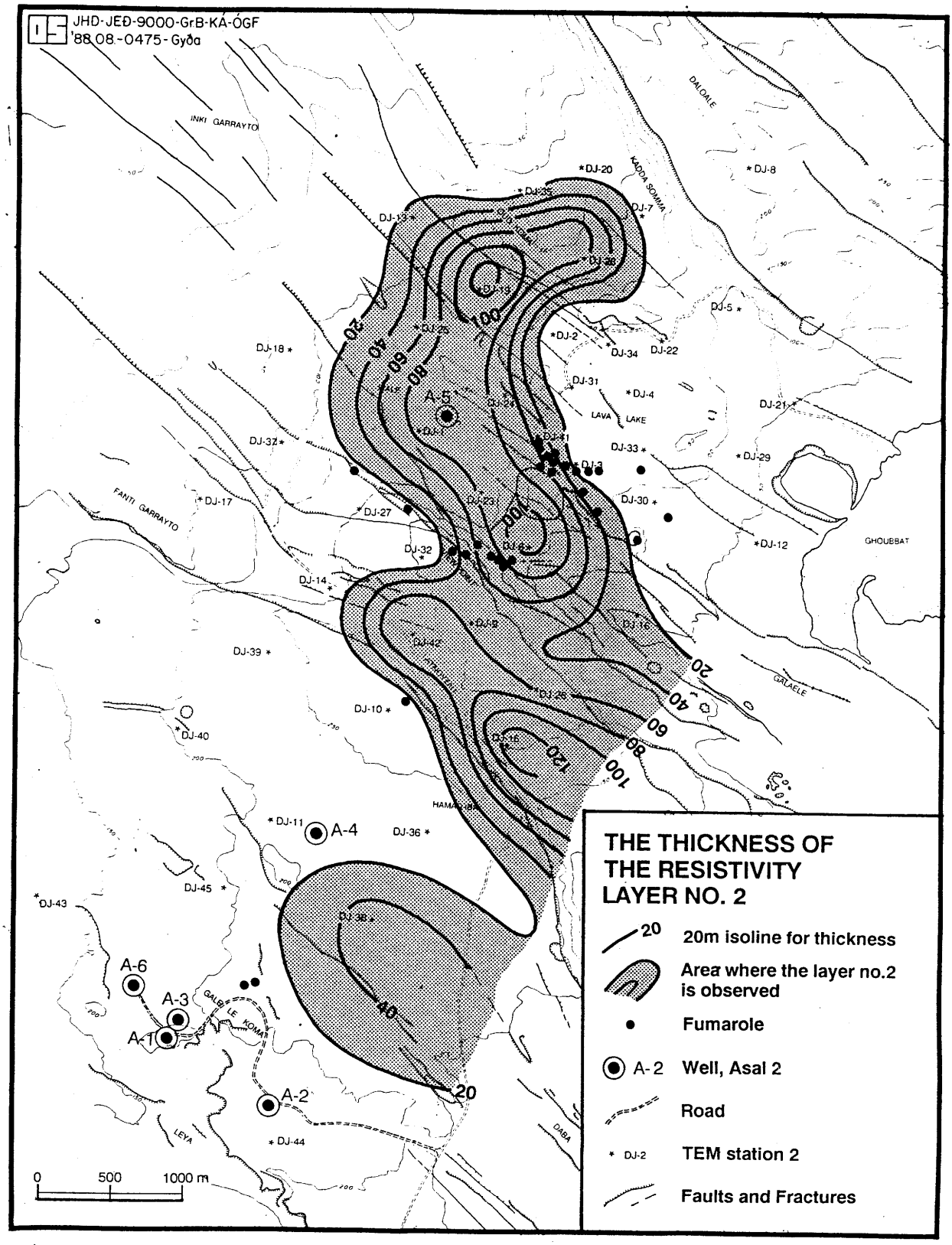


**Figure 2.** The extent and thickness of resistivity layer 2.

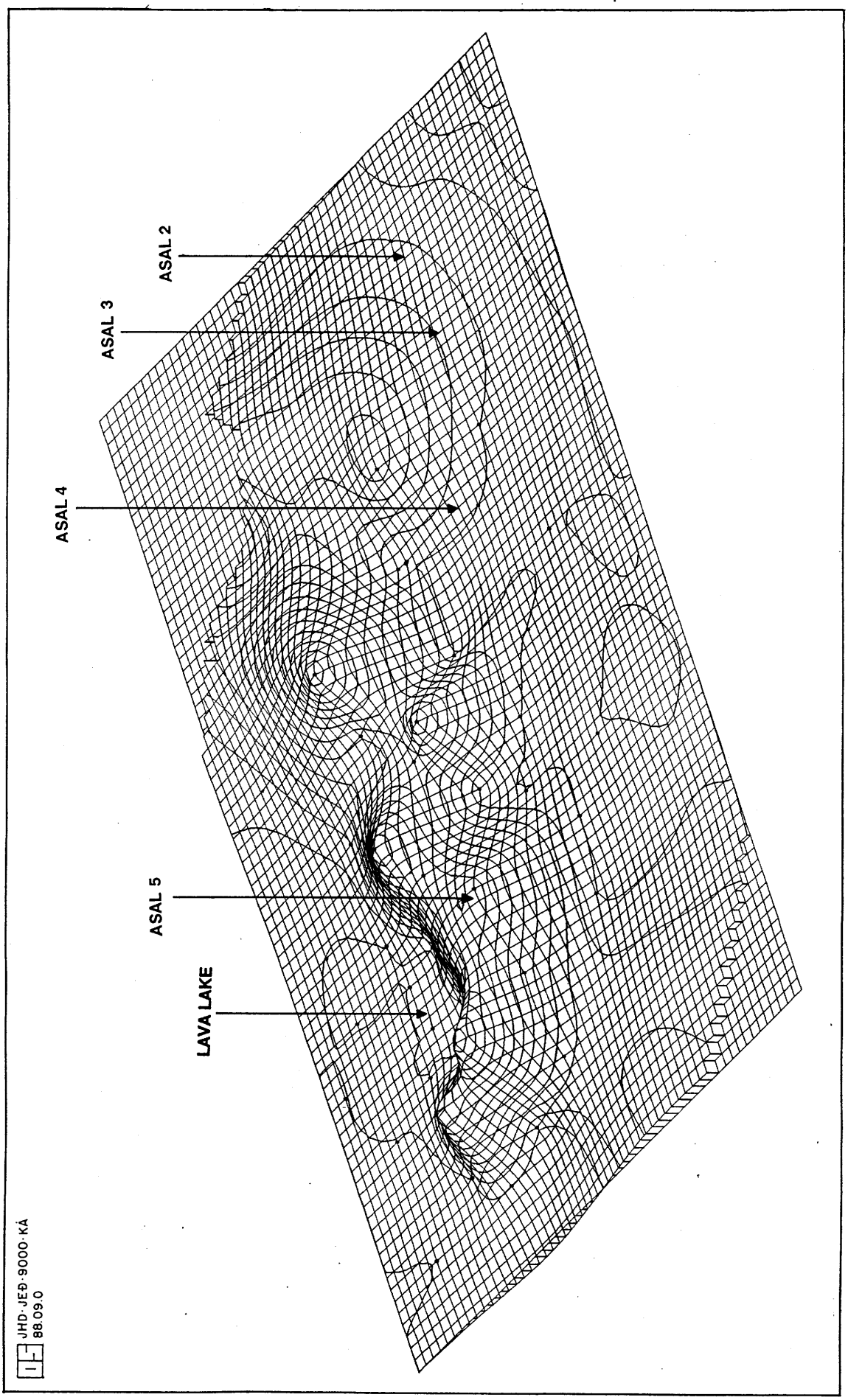


**Figure 3.** A three dimensional view of the thickness of layer 2.

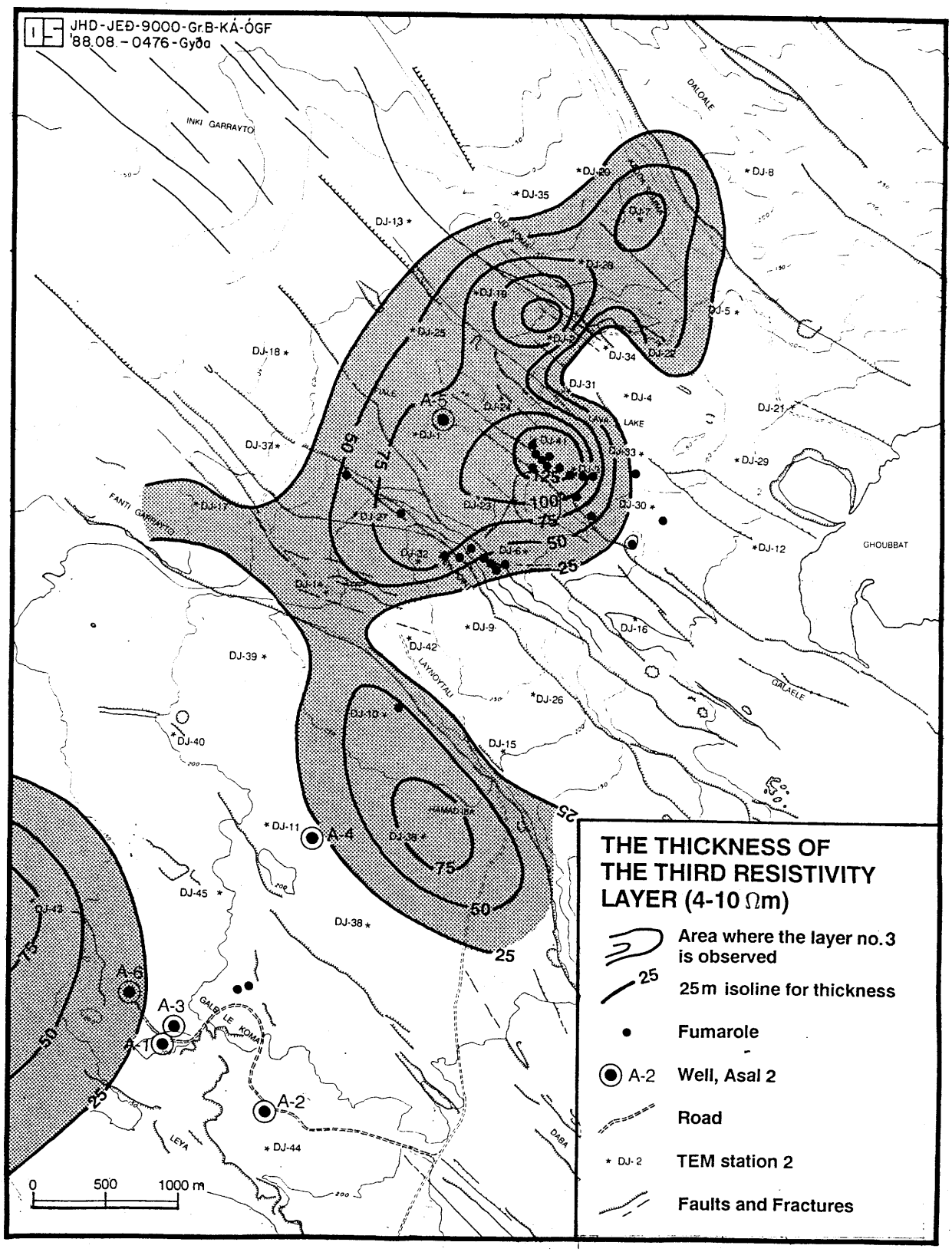


**Figure 4.** The extent and the thickness of resistivity layer 3.

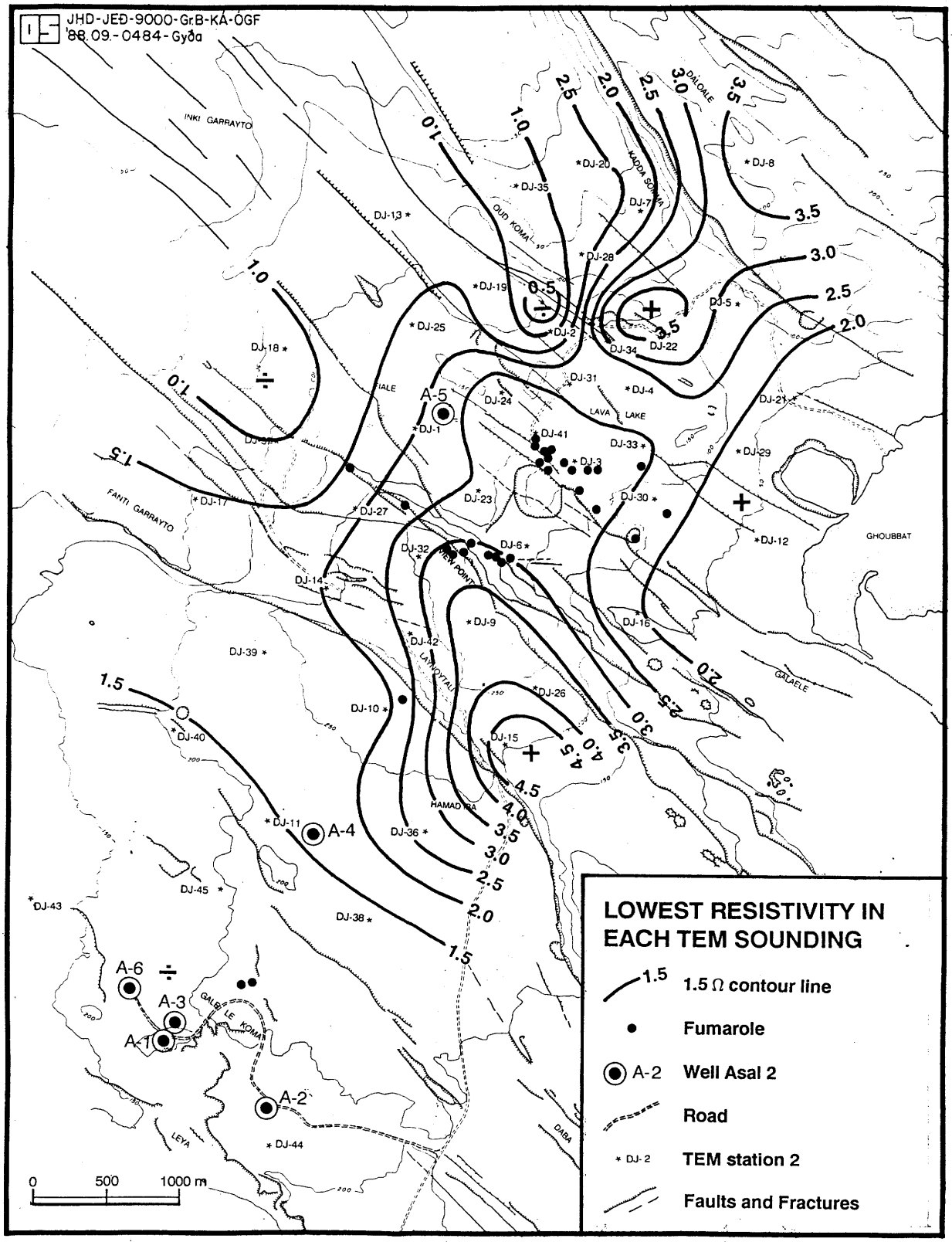


**Figure 5.** Map of the lowest resistivity in layers 4 and 5.

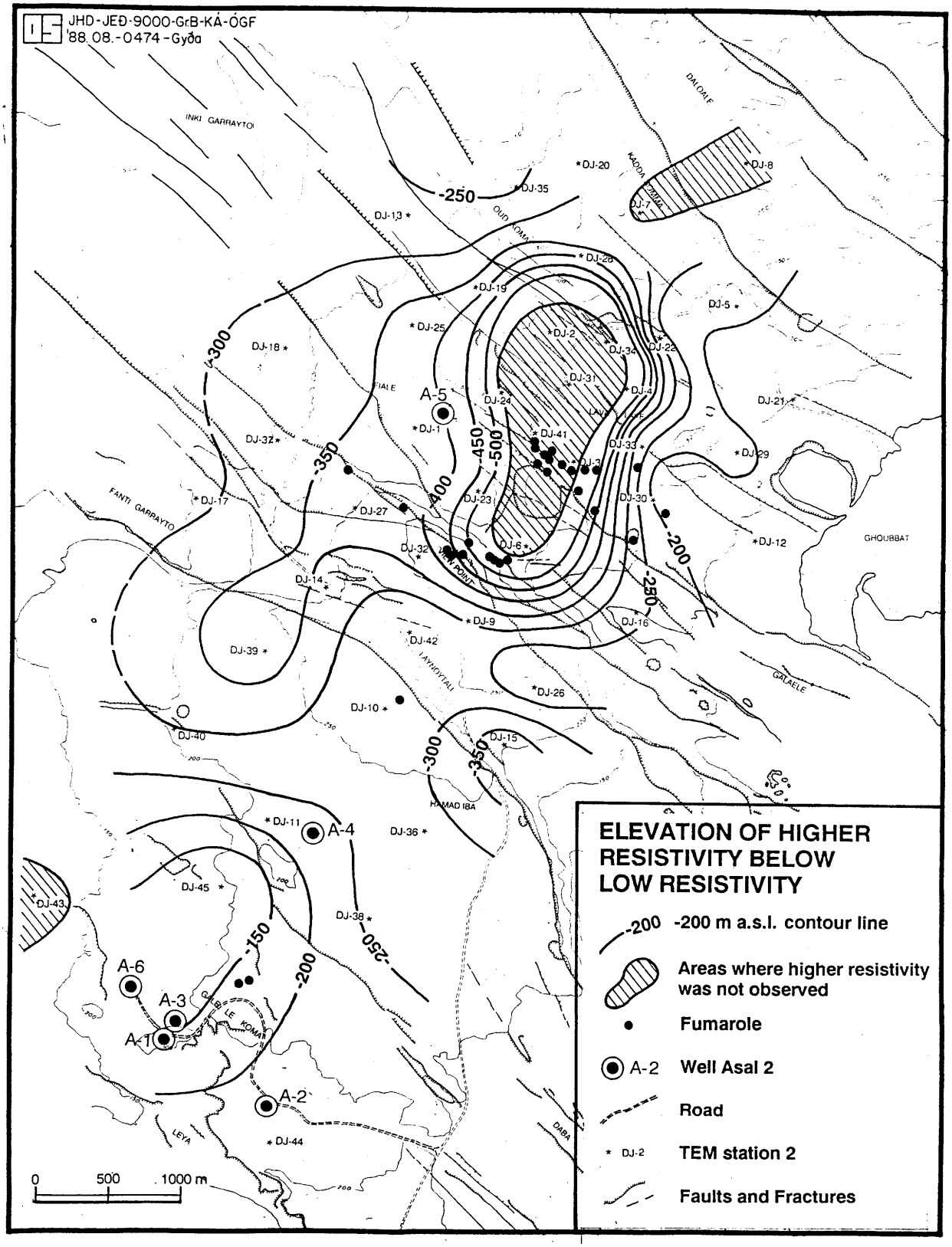


**Figure 6.** The elevation of the top of the resistivity layer 6 (the high resistivity layer).

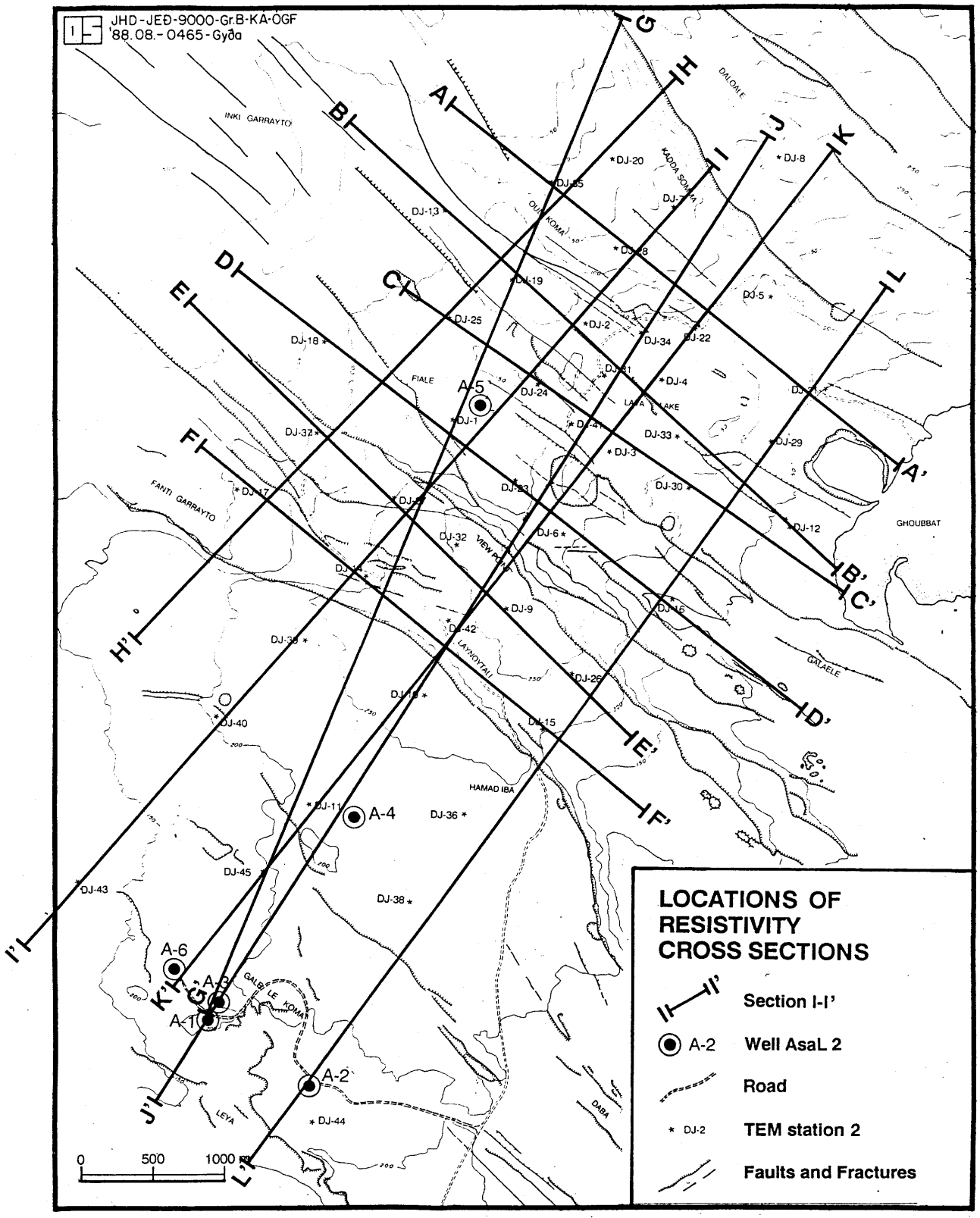


**Figure 7.** The location of the resistivity cross-sections.

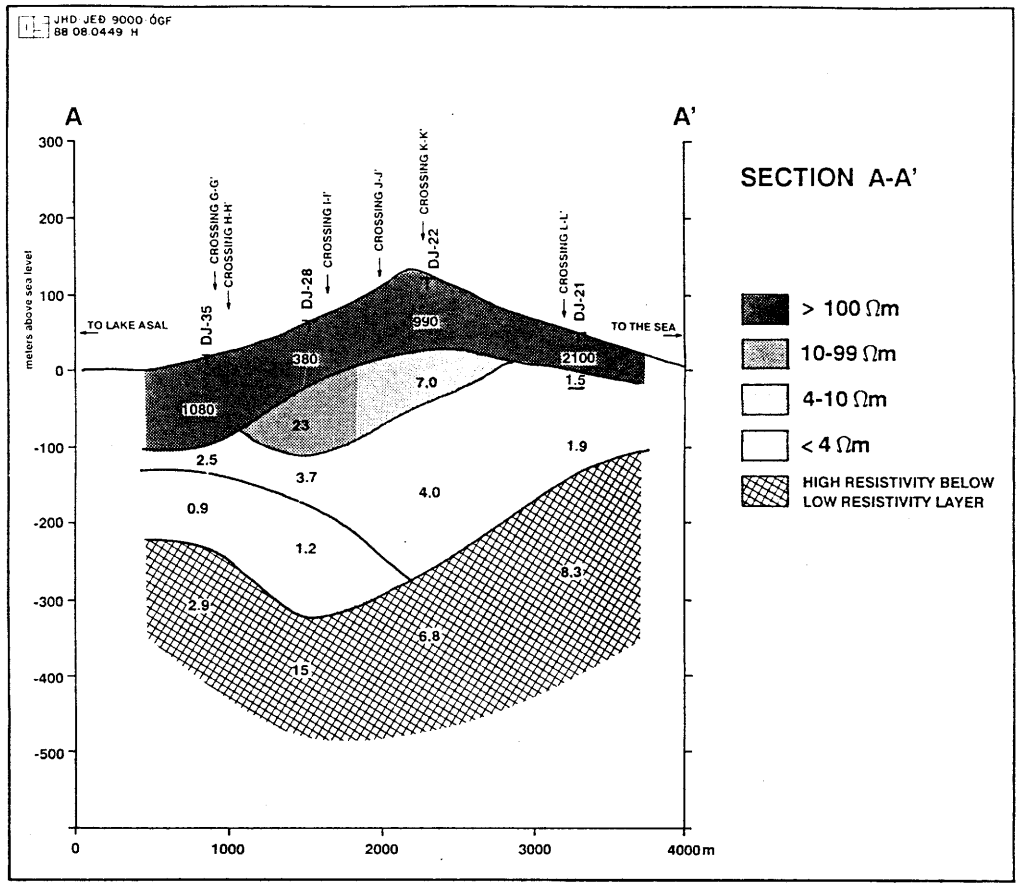


**Figure 8.** Resistivity cross-section AA'

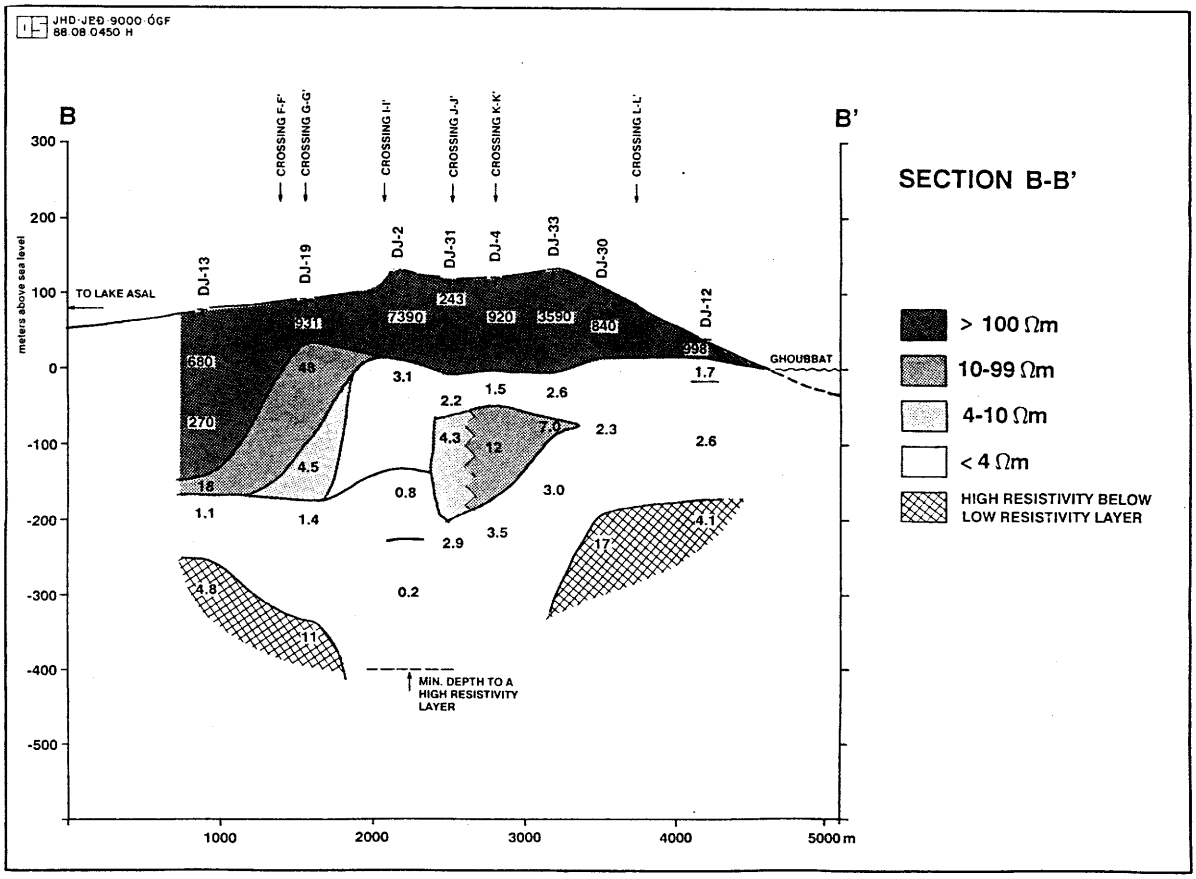


**Figure 9.** Resistivity cross-section BB'

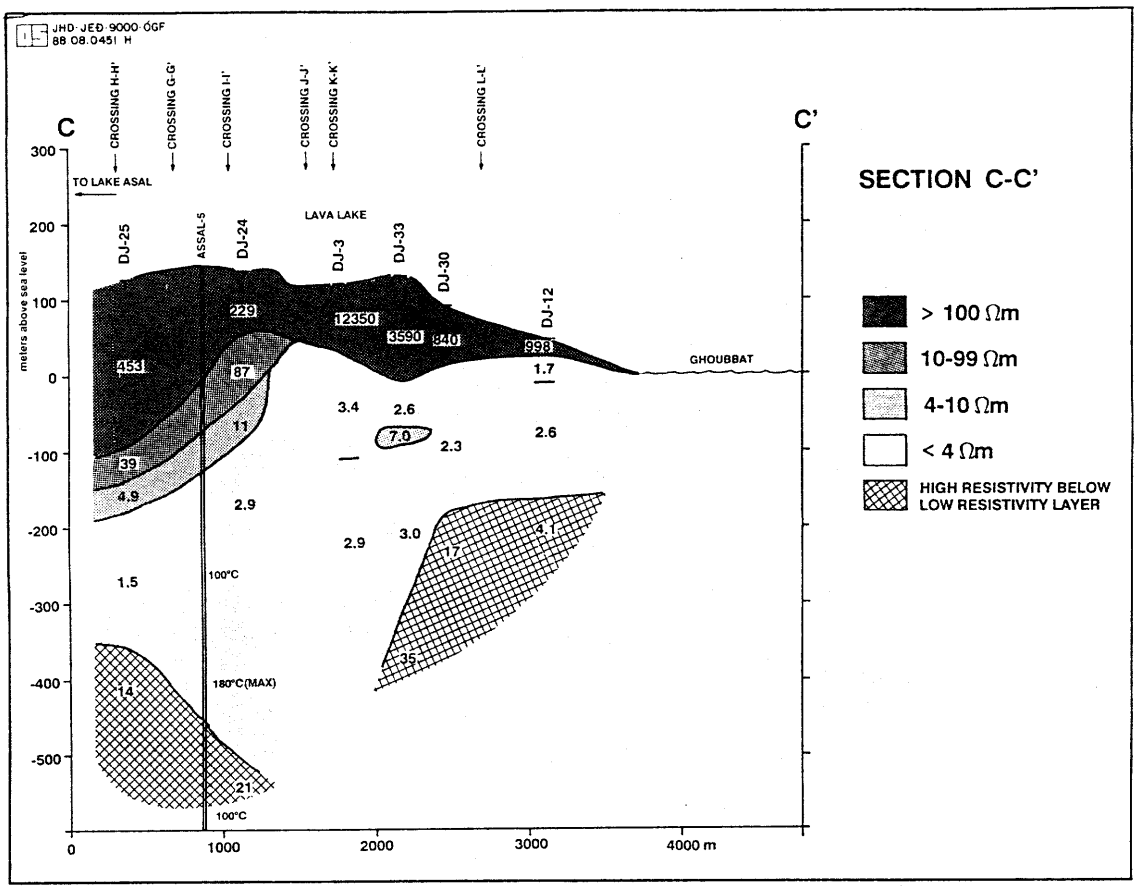


**Figure 10.** Resistivity cross-section CC'

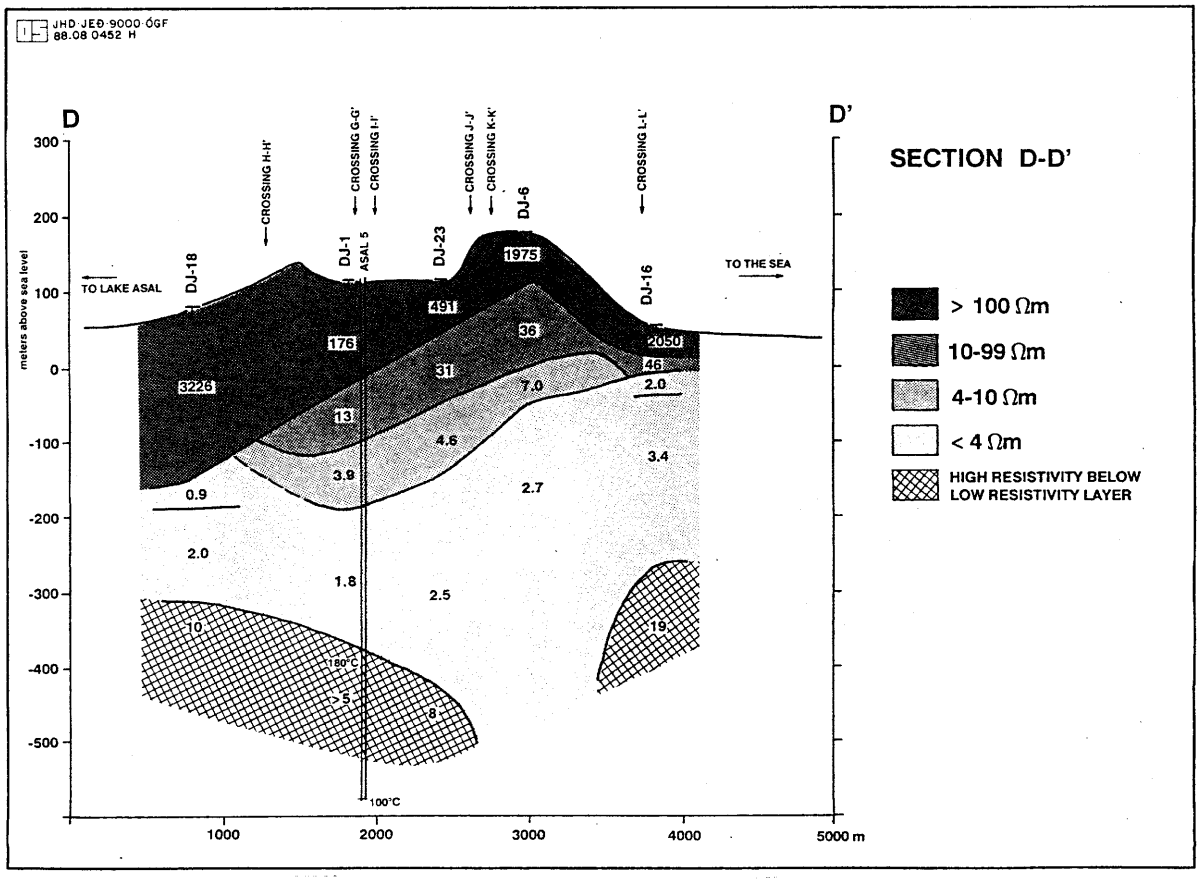


**Figure 11.** Resistivity cross-section DD'

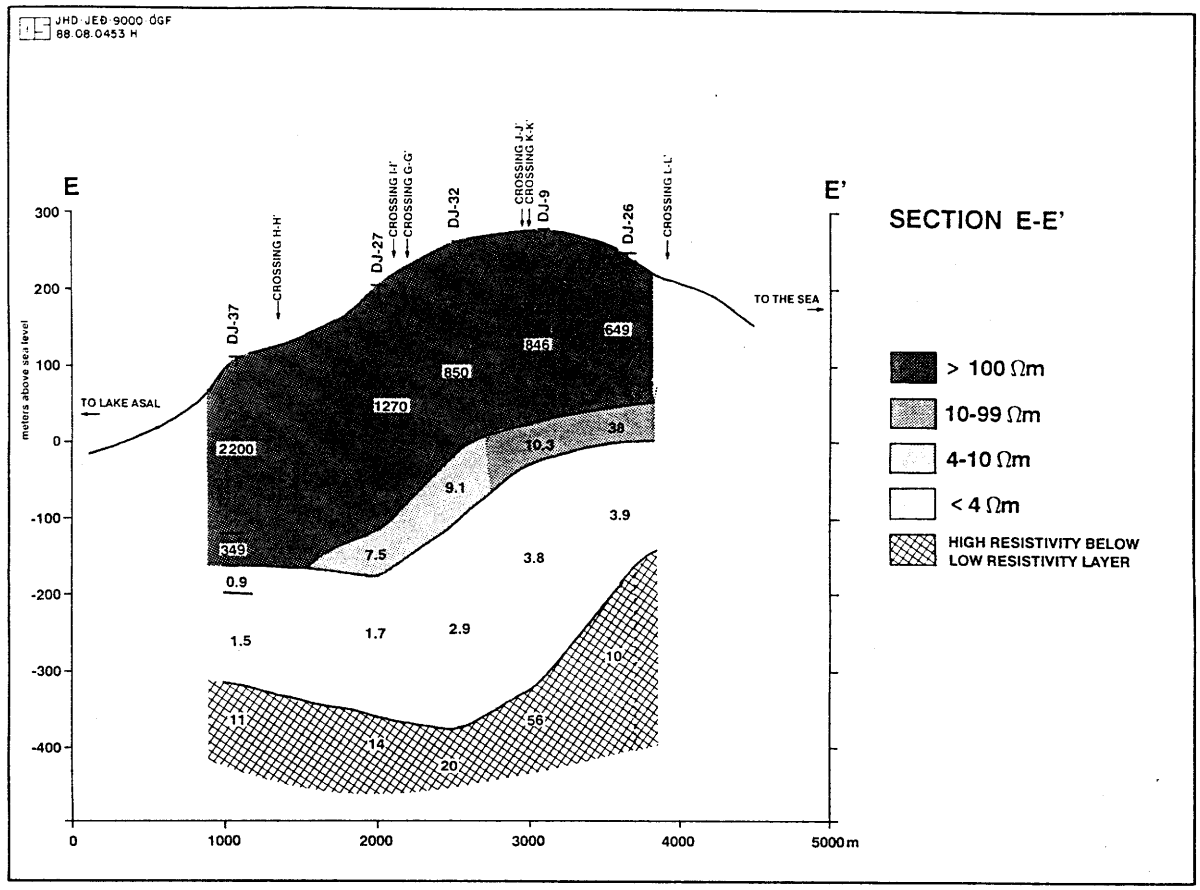


**Figure 12.** Resistivity cross-section EE'

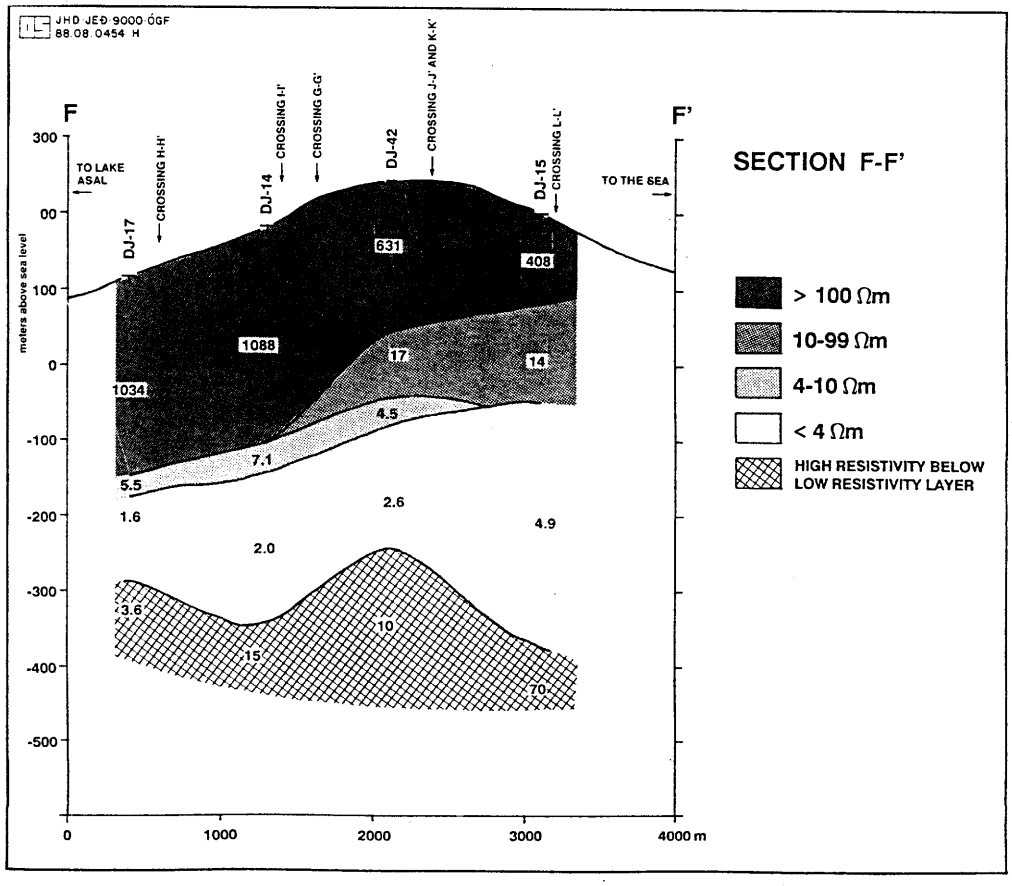


**Figure 13.** Resistivity cross-section FF'

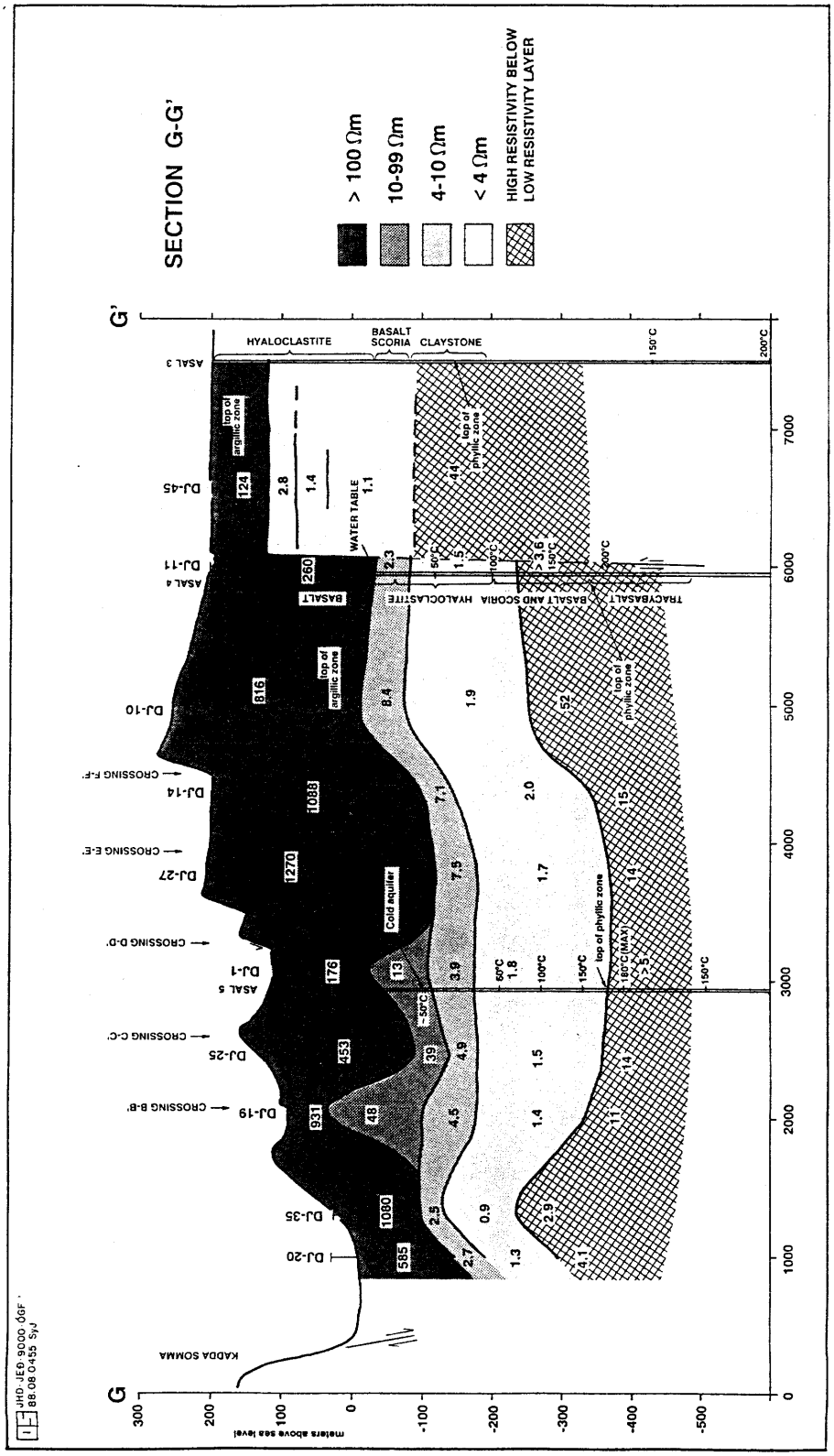


**Figure 14.** Resistivity cross-section GG'

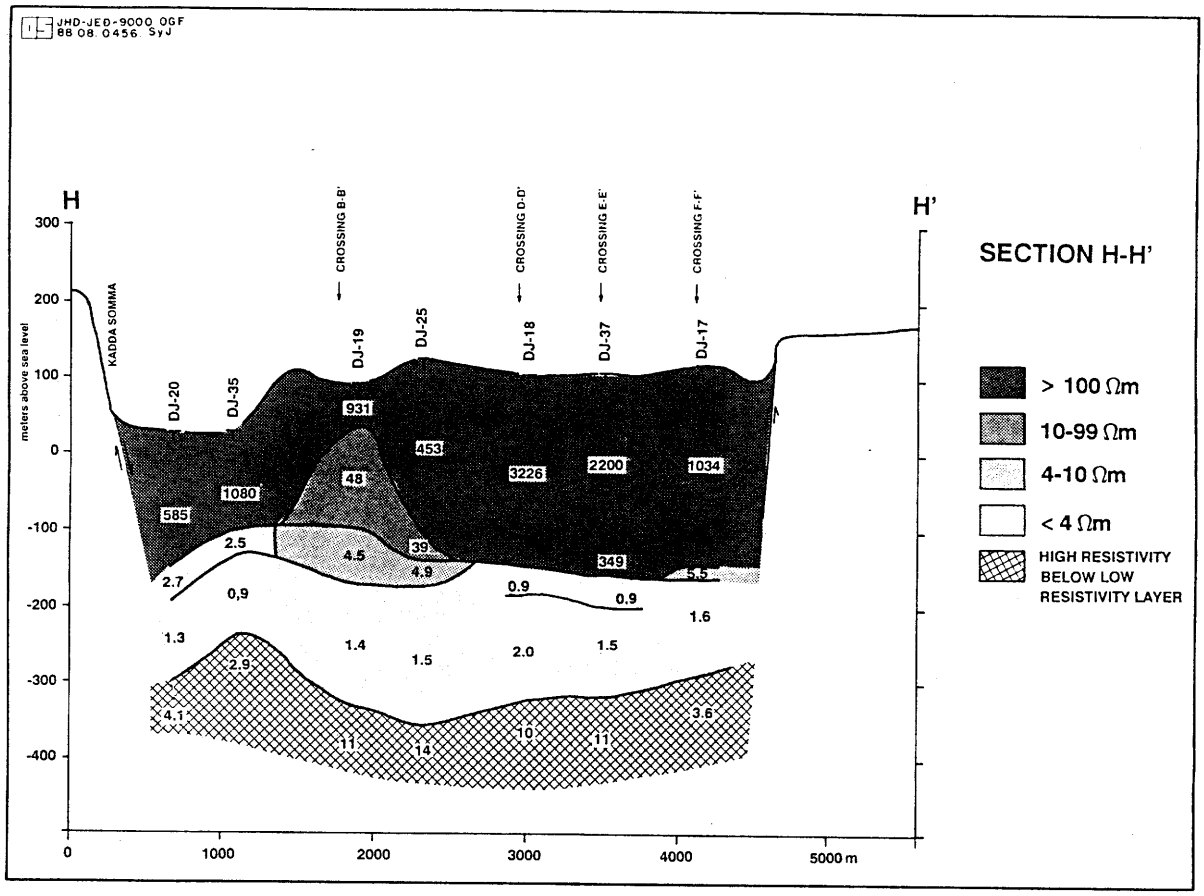


**Figure 15.** Resistivity cross-section HH'

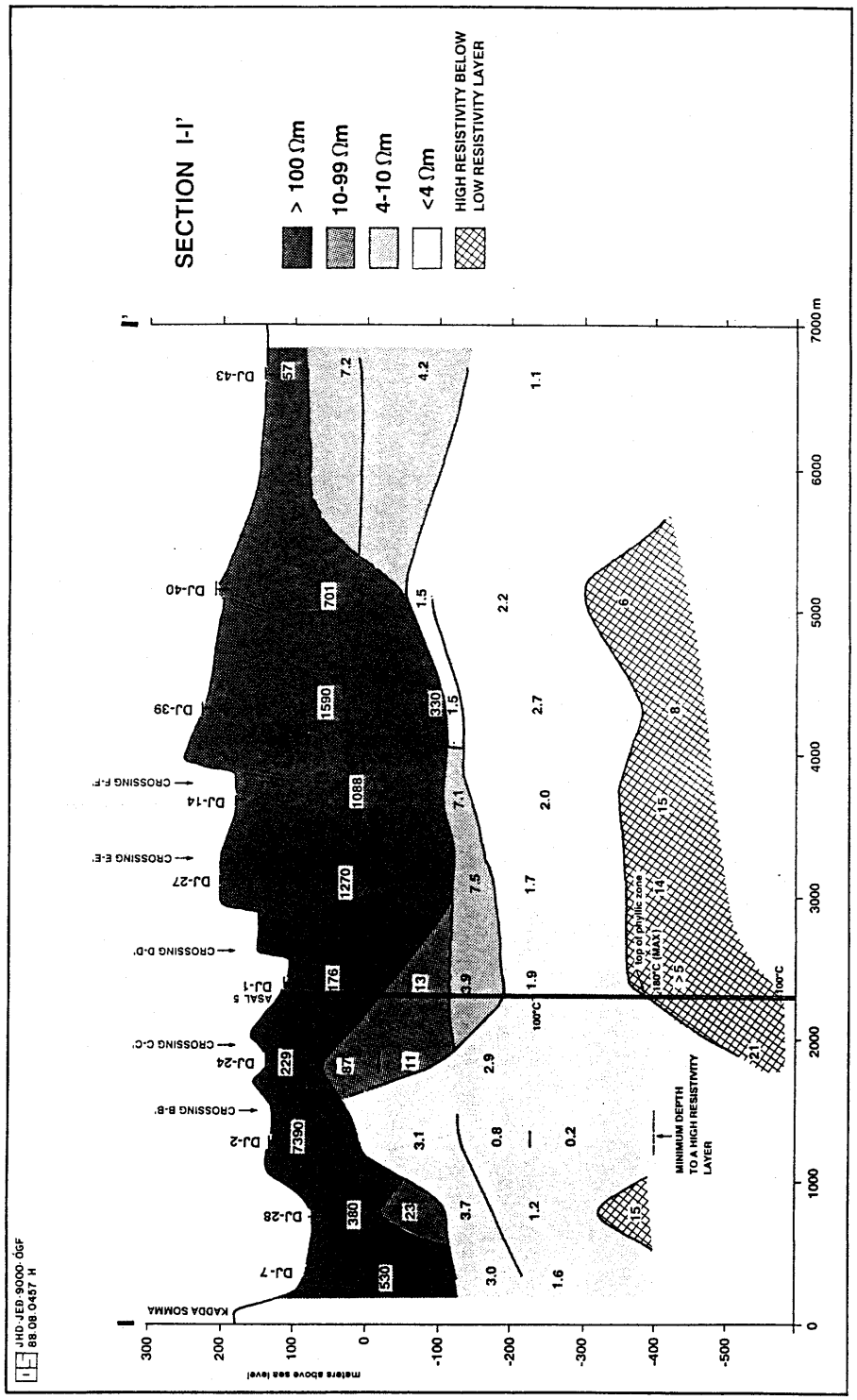


**Figure 16.** Resistivity cross-section II'

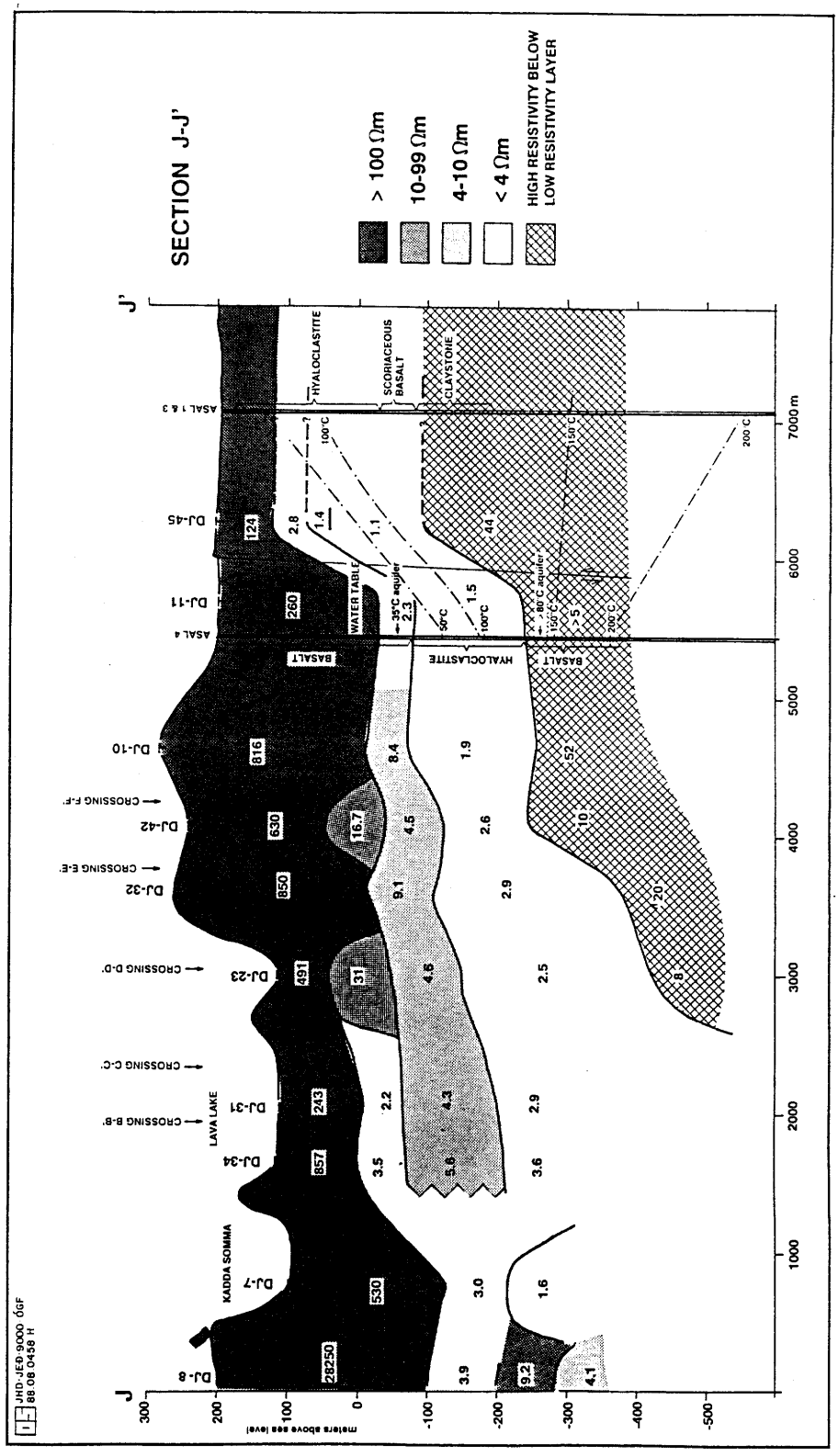


**Figure 17.** Resistivity cross-section JJ'

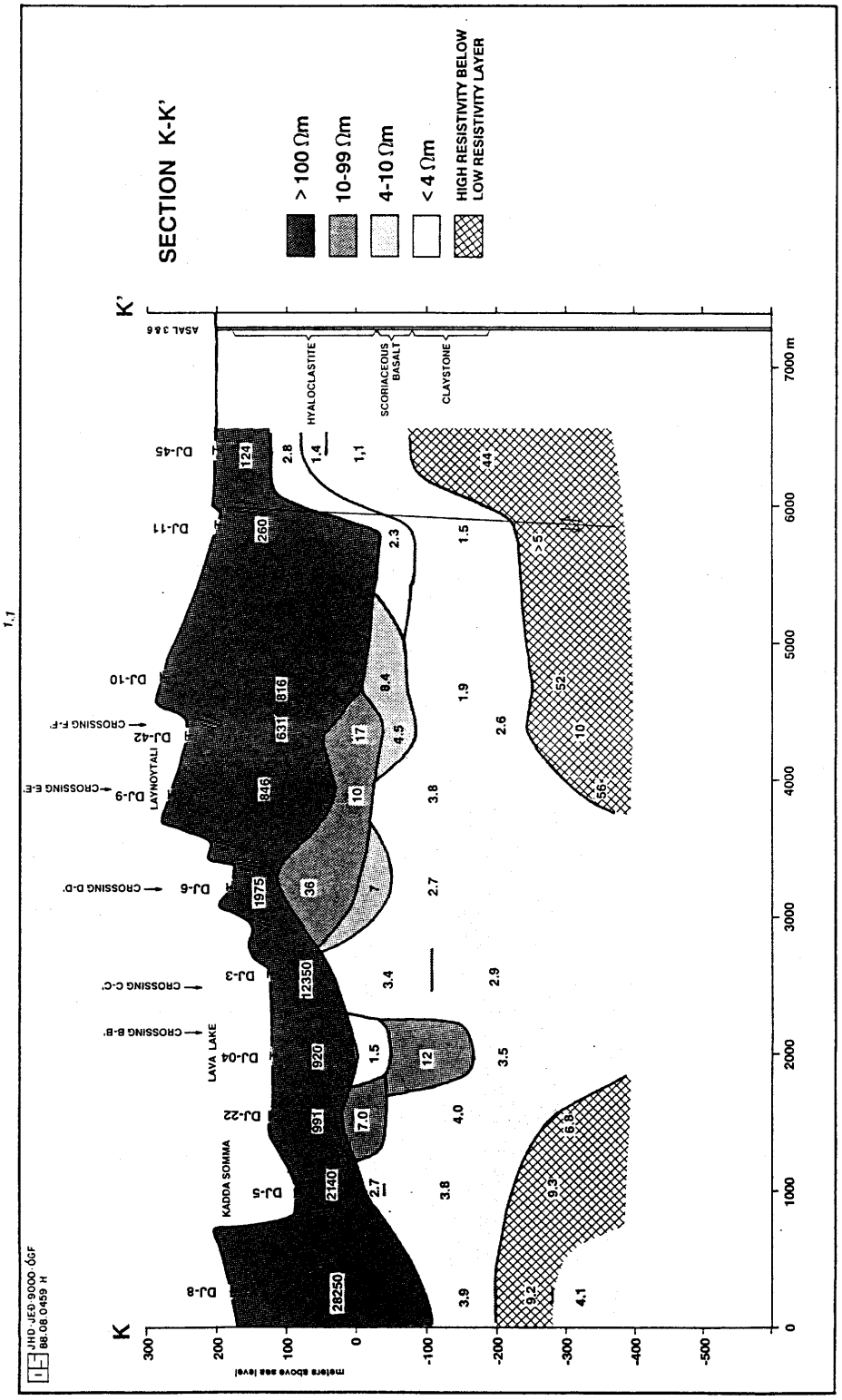


**Figure 18.** Resistivity cross-section KK'

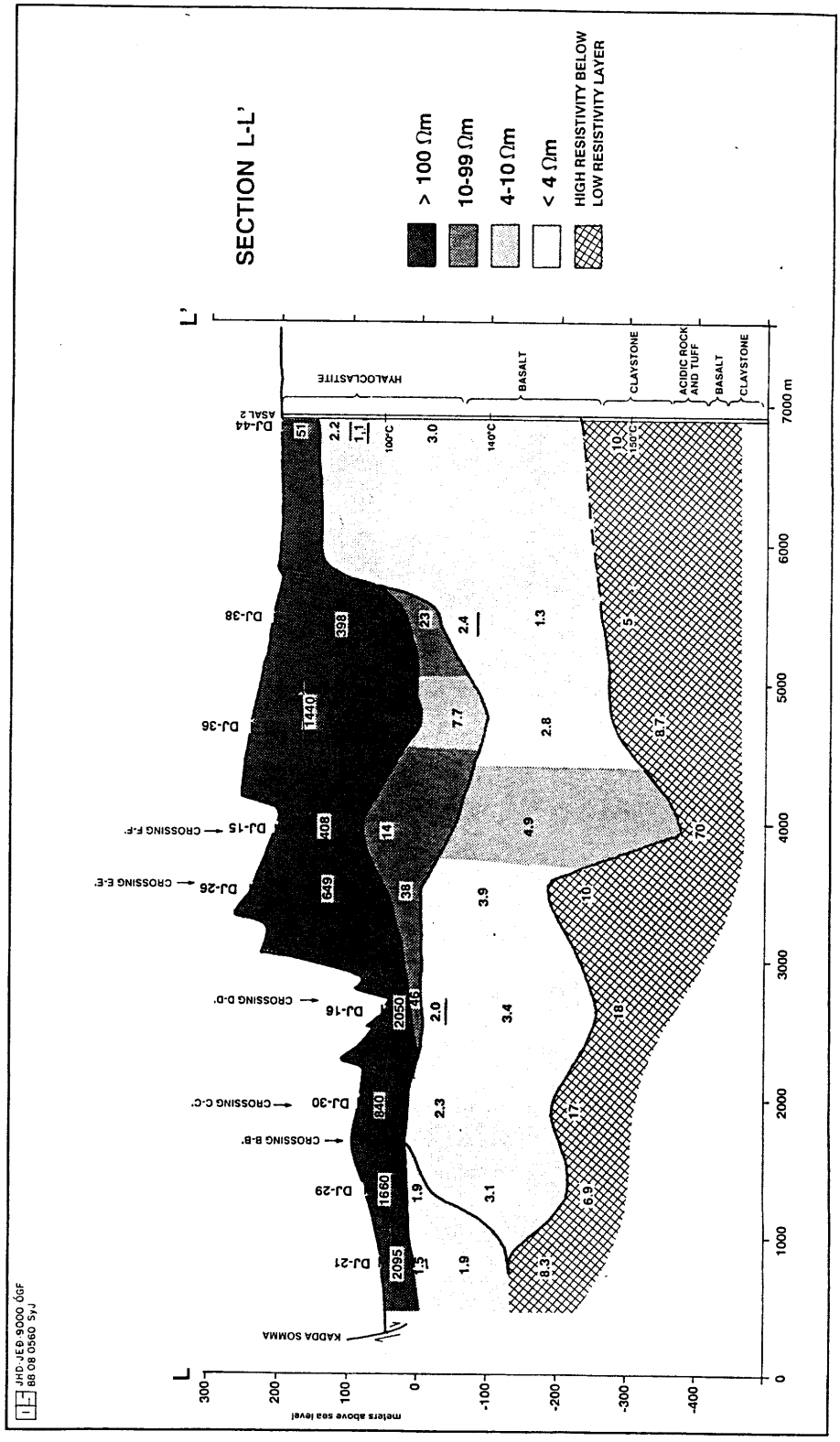


**Figure 19.** Resistivity cross-section LL'

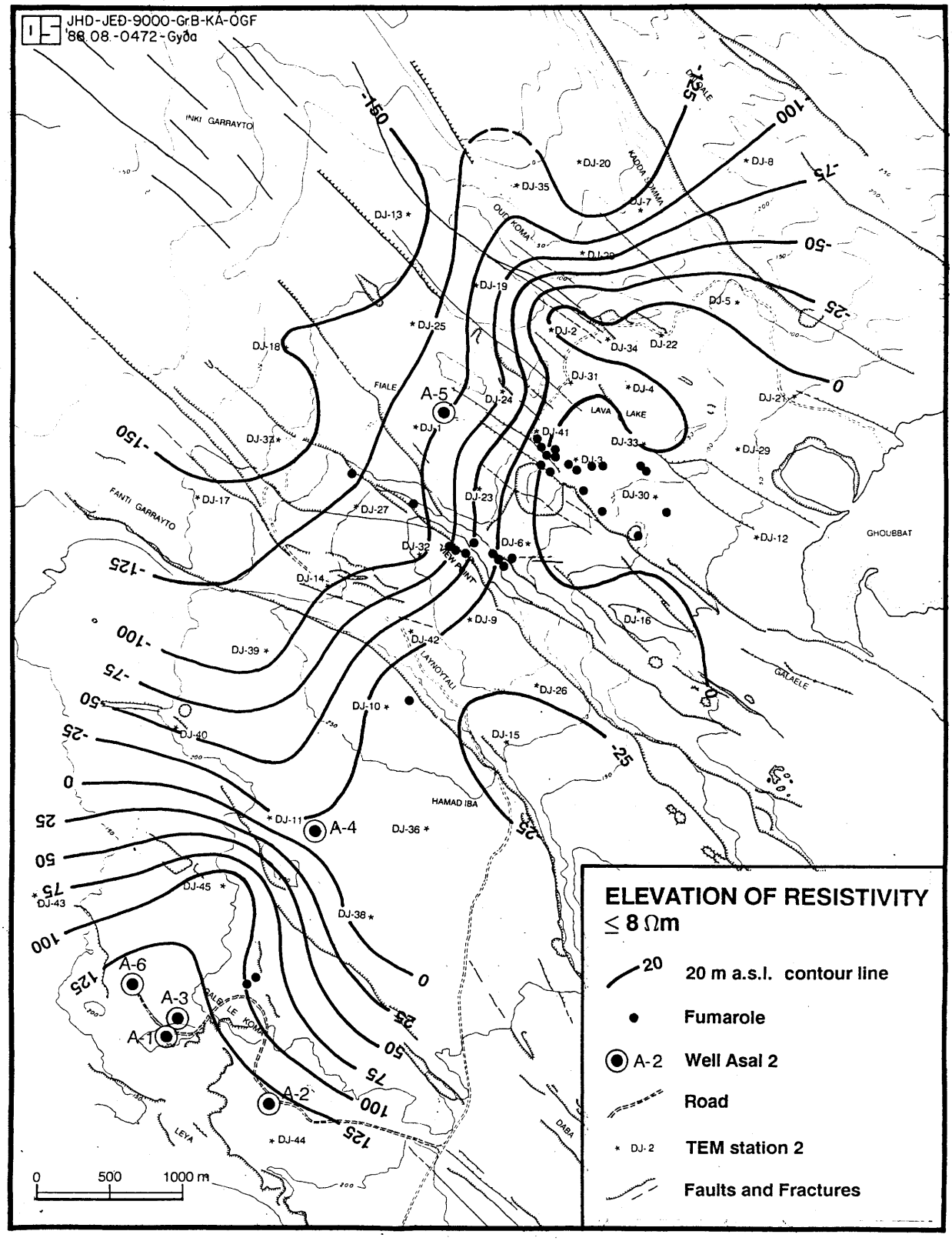


**Figure 20.** The elevation of the water table.

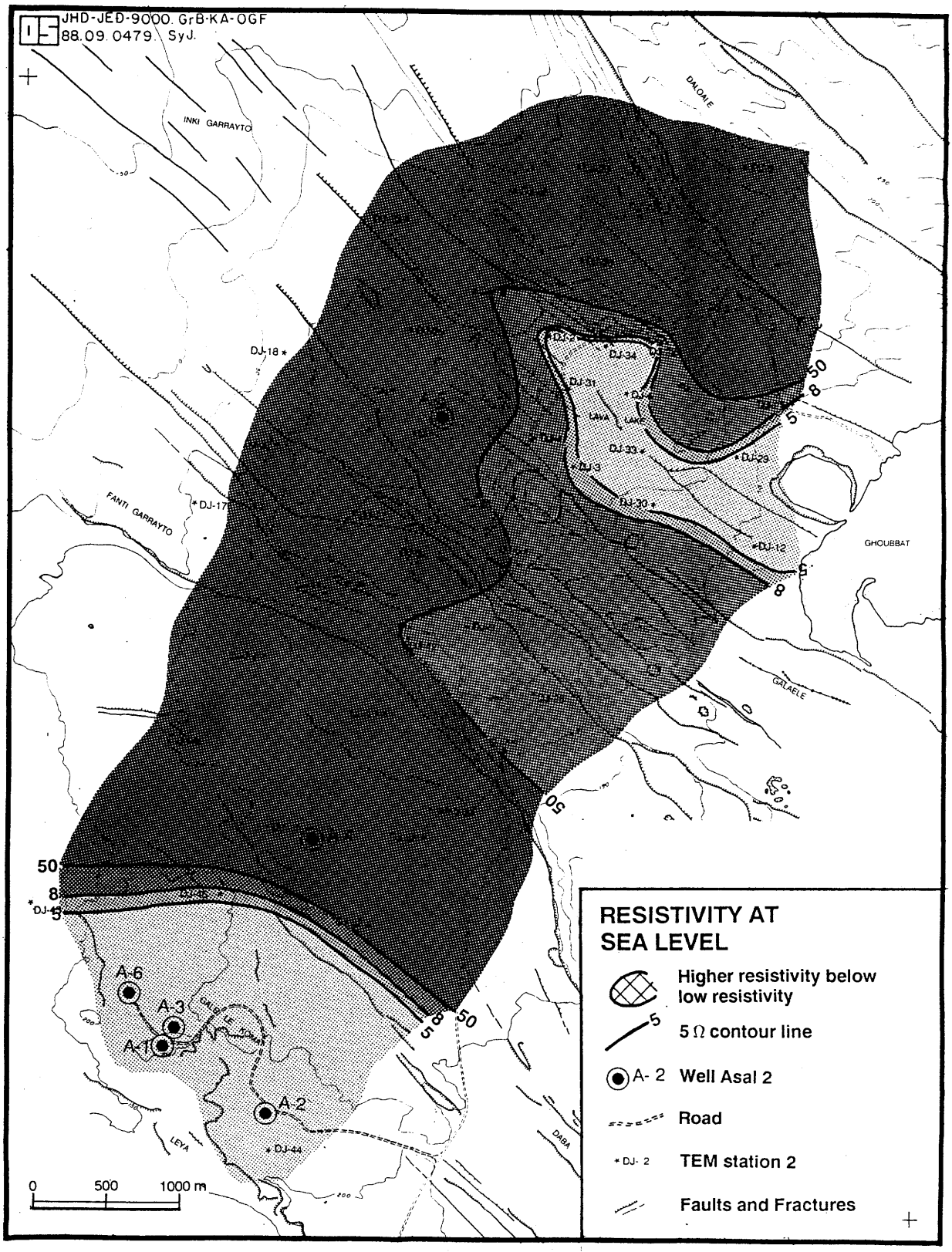


**Figure 21.** The resistivity at sea level

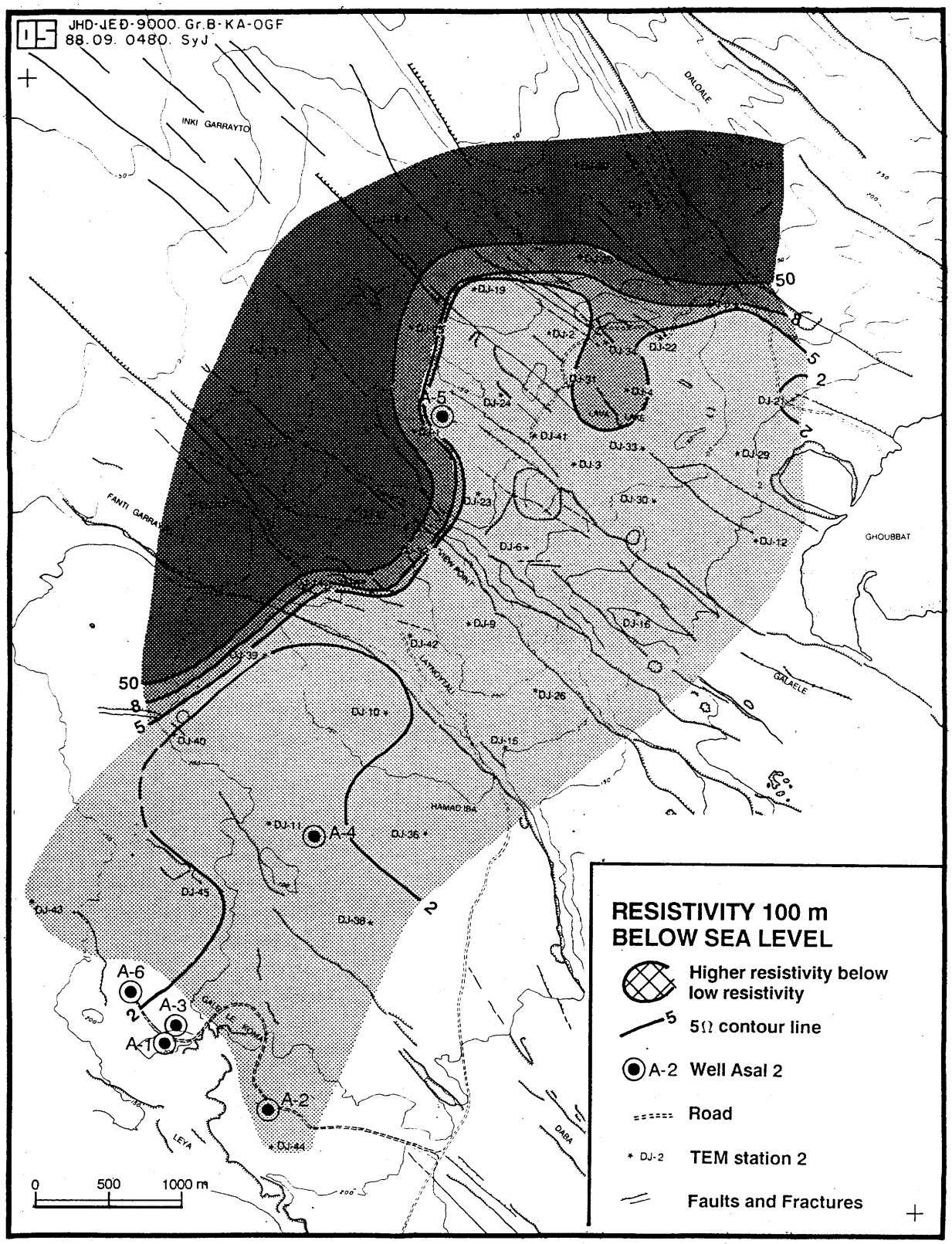


**Figure 22.** The resistivity at 100 m depth below sea level

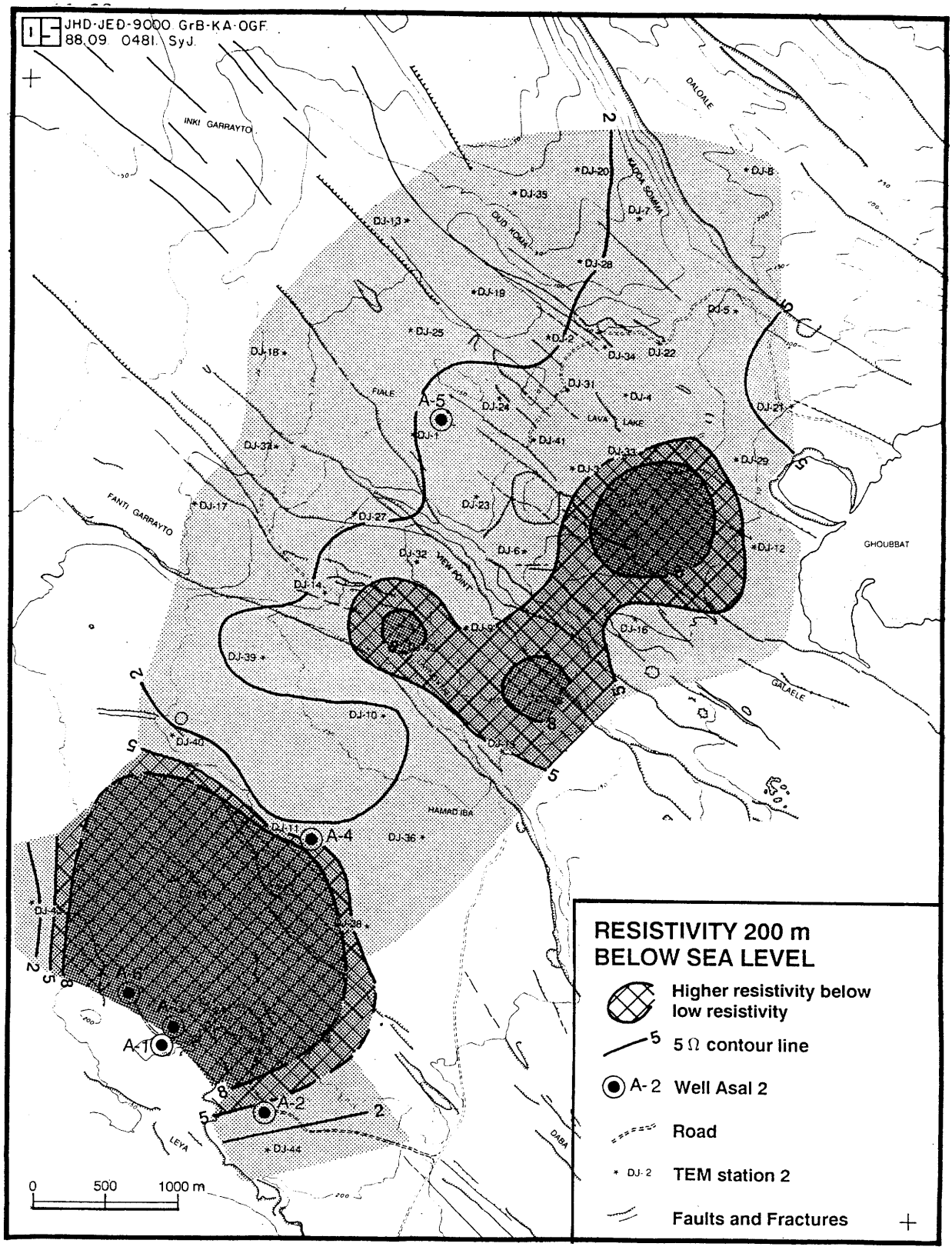


**Figure 23.** The resistivity at 200 m depth below sea level

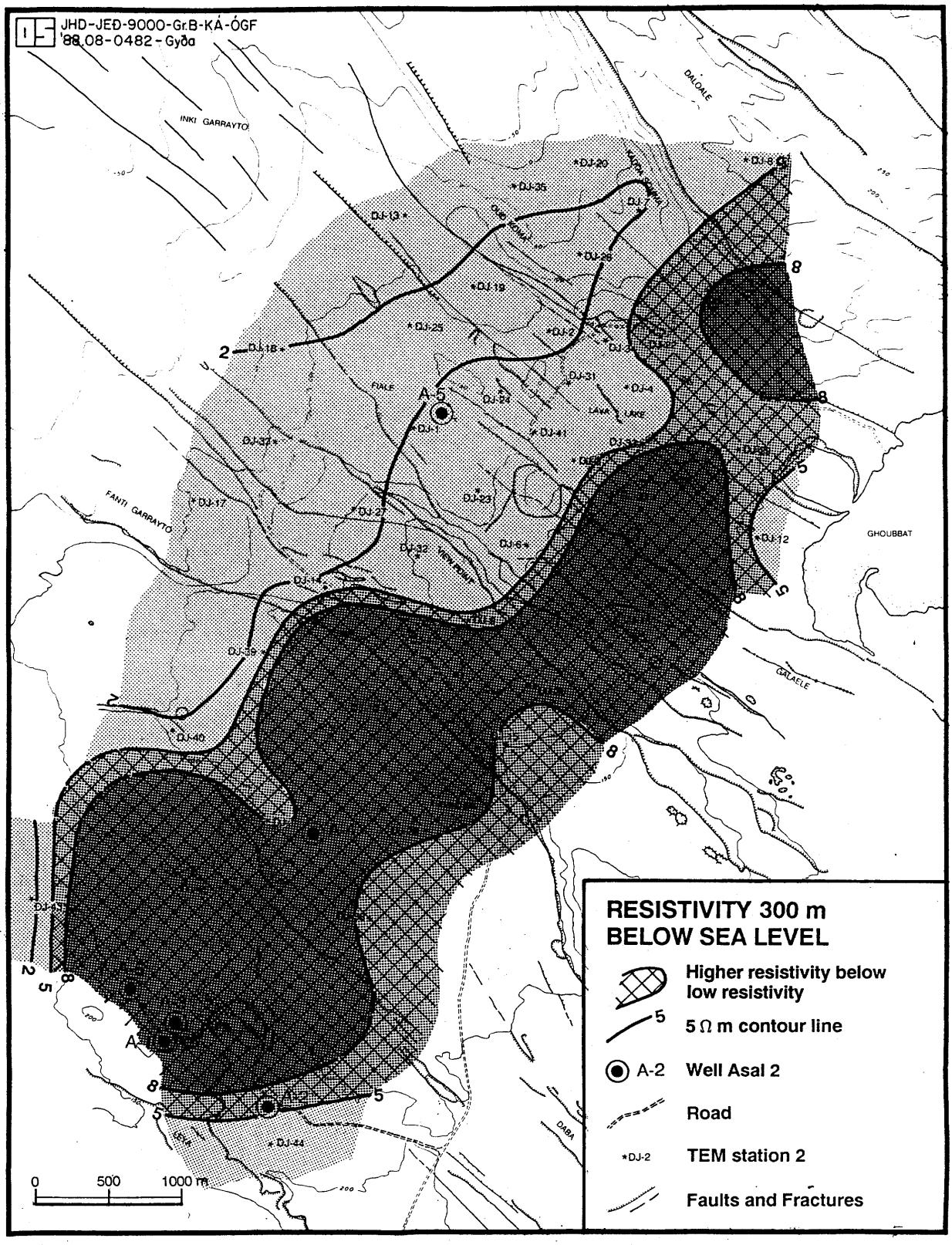


**Figure 24.** The resistivity at 300 m depth below sea level

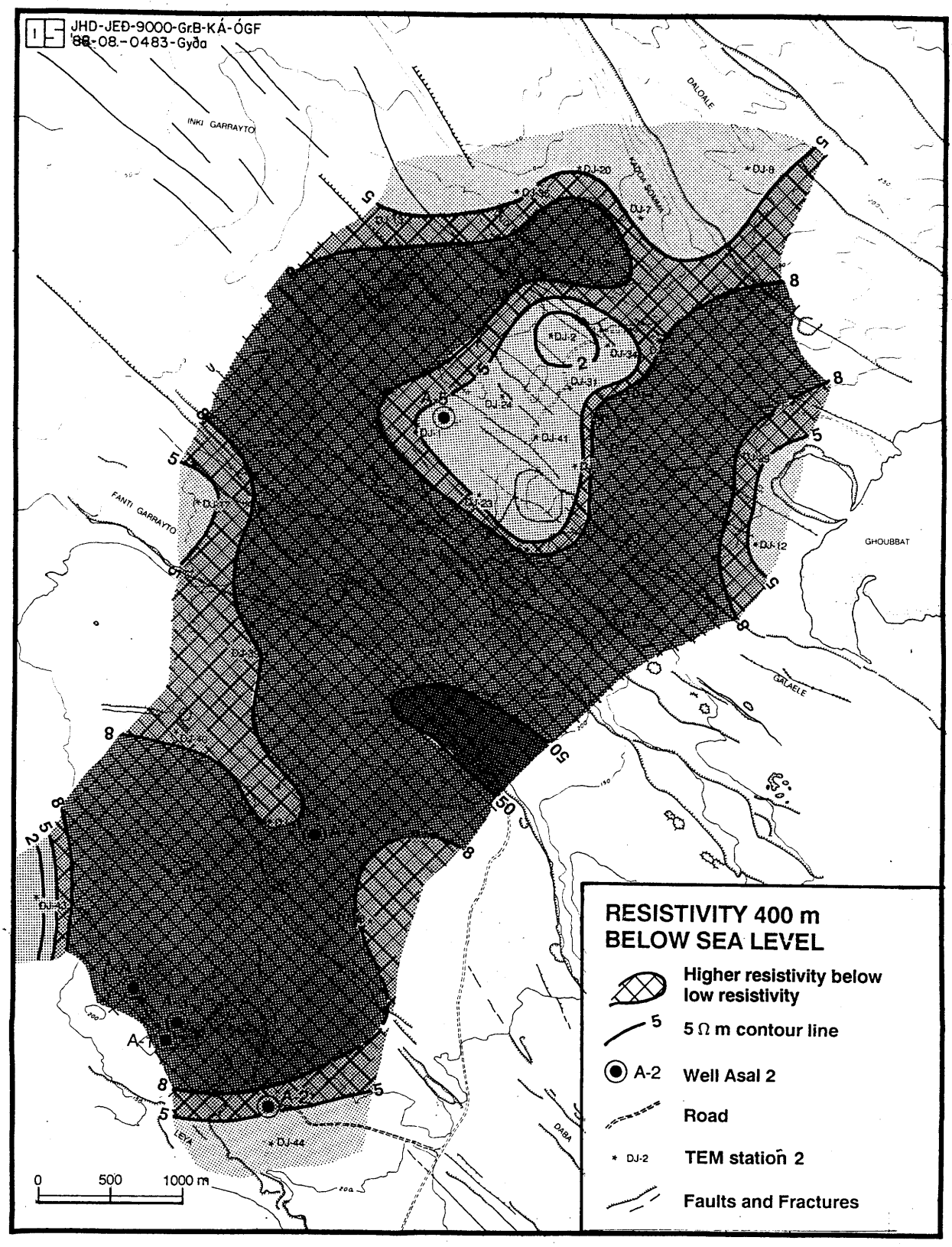


**Figure 25.** The resistivity at 400 m depth below sea level